



HAL
open science

Hybrid Modeling for In Situ Artificial Fish Spawning Ground Stabilization

Kim-jehanne Lupinski, Guillaume Brousse, Raphael Maurin, Pierre Sagnes,
Dominique Courret, Laurent Lacaze, Magali Jodeau, Florian Cordier

► **To cite this version:**

Kim-jehanne Lupinski, Guillaume Brousse, Raphael Maurin, Pierre Sagnes, Dominique Courret, et al.. Hybrid Modeling for In Situ Artificial Fish Spawning Ground Stabilization. River Research and Applications, In press, 10.1002/rra.4403 . hal-04892356

HAL Id: hal-04892356

<https://hal.science/hal-04892356v1>

Submitted on 16 Jan 2025

HAL is a multi-disciplinary open access archive for the deposit and dissemination of scientific research documents, whether they are published or not. The documents may come from teaching and research institutions in France or abroad, or from public or private research centers.

L'archive ouverte pluridisciplinaire **HAL**, est destinée au dépôt et à la diffusion de documents scientifiques de niveau recherche, publiés ou non, émanant des établissements d'enseignement et de recherche français ou étrangers, des laboratoires publics ou privés.



Distributed under a Creative Commons Attribution - NonCommercial - NoDerivatives 4.0
International License

RESEARCH ARTICLE OPEN ACCESS

Hybrid Modeling for In Situ Artificial Fish Spawning Ground Stabilization

Kim-Jehanne Lupinski^{1,2}  | Guillaume Brousse^{1,2} | Raphaël Maurin^{3,4} | Pierre Sagnes^{4,5}  | Dominique Courret^{4,5} | Florian Cordier¹ | Laurent Lacaze^{3,4} | Magali Jodeau^{1,2}

¹Laboratoire National d'Hydraulique et Environnement (LNHE), EDF R&D, Chatou, France | ²Laboratoire d'Hydraulique Saint-Venant (LHSV), École des Ponts ParisTech | EDF R&D, Chatou, France | ³Institut de Mécanique des Fluides de Toulouse (IMFT), UMR 5502, Toulouse, France | ⁴Pôle R&D 'Ecohydraulique', OFB-IMFT-PPRIME, Toulouse, France | ⁵Direction de la Recherche et de l'Appui Scientifique, Office Français de la Biodiversité (OFB), Toulouse, France

Correspondence: Kim-Jehanne Lupinski (kim-jehanne.lupinski@edf.fr)

Received: 17 January 2024 | **Revised:** 30 October 2024 | **Accepted:** 4 November 2024

Funding: This work was supported by ANR project 15-CE01-0013 SEDIFLO.

Keywords: bedload | dams | numerical modeling | physical modeling | Salmonid species | sediment replenishment | spawning ground restoration

ABSTRACT

Erosion generally reduces the resilience of replenished gravel in rivers. As a result, structures are sometimes added to modify the upstream flow and stabilize artificial spawning grounds. In particular, rows of boulders can be placed around the replenishment area to limit the transport of replenished gravel during flood events. This study aims to optimize the arrangement of these rows, based on field experiments as well as physical and numerical models. A combined hydro-sedimentary numerical model is calibrated and validated by comparing simulated and measured morphological evolutions in nine laboratory experiments. The results show that boulders positioned downstream of the replenishment slow down the flow above the replenishment, decreasing shear stress over the gravel. The stabilization efficiency depends on both the positioning of the boulders and the arrangement of the replenished surface. To achieve sustainable spawning, prospective scenarios using the numerical model highlight the need to limit the width of the replenishment area. Experiments demonstrated that when the replenishment area spans the entire width flume, the erosion rate is significantly higher compared to a narrower replenishment area placed close to the edges. This effect is attributed to increased flow velocities in the center of the channel, leading to increased shear stress and gravel erosion.

1 | Introduction

Spawning grounds are of utmost importance for lithophilic fish species, as they support breeding capacity and egg incubation (Beechie et al. 2005; Beschta and Platts 1986; Geist and Dauble 1998). Characteristics defining the functionality of spawning grounds are specific to fish species. Lithophilic habitats, especially those used by Salmonids, are mainly composed of gravel. Kondolf and Wolman (1993) demonstrated that Salmonids can spawn in gravel with a median diameter up to about 10% of their body length. In rivers, sediment characteristics and mobility depend on the hydromorphological

context of the watershed, such as geology and anthropic activities. Sustainability of the spawning habitats is determined by the capacity of the hydrosystem to provide sufficient sediment supply and appropriate hydraulic conditions. In addition to factors like temperature and pollution, sustainable spawning relies on sediment continuity. However, downstream of dams with large reservoirs, water, and sediment supply are regulated, leading river morphologies to adapt to a new equilibrium (Brandt 2000; Petts 1984). Disturbances in sedimentary equilibrium can result in channel degradation and narrowing, bed armoring, and increased vegetation growth on alluvial bars. Overall, the riverbed can be significantly

This is an open access article under the terms of the [Creative Commons Attribution-NonCommercial-NoDerivs](https://creativecommons.org/licenses/by-nc-nd/4.0/) License, which permits use and distribution in any medium, provided the original work is properly cited, the use is non-commercial and no modifications or adaptations are made.

© 2024 The Author(s). *River Research and Applications* published by John Wiley & Sons Ltd.

eroded, or the sediment grain size can coarsen, leading to bed armoring and degradation of spawning grounds (Brenna, Surian, and Mao 2020; Surian and Rinaldi 2003; Williams and Wolman 1984). A strong correlation has been recognized between the loss of spawning grounds and the decline or disappearance of economically significant fish species, such as Salmonids (Kondolf 1997).

The long history of spawning ground restoration in the literature (Roni et al. 2014; Thompson 2006) underlines its global importance. Sediment replenishment, also known as gravel augmentation, involves the artificial injection of gravel to counteract the lack of natural bed material from upstream sources (Mörtl and De Cesare 2021). Two types of replenishment may be used, depending on the objectives of restoration and the morphological context. The first method restores sediment stocks in the active channel, allowing the flow to transport sediment and form new riverbed material (Arnaud et al. 2017; Brousse et al. 2020; Ock, Sumi, and Takemon 2013). Since this is a process-based strategy, it may require a long time and significant amounts of sediment to restore fish habitats. The second approach focuses on adapting the local shape of artificial spawning areas to specific fish species, including gravel size, thickness, and coverage area (Bunte 2004). This form-based strategy requires less sediment, enabling quicker restoration of artificial spawning grounds (Whiteway et al. 2010). Artificial spawning areas have been created in many Salmonid rivers (Kondolf et al. 2014; Staentzel et al. 2020). Harrison et al. (2019) showed that the texture and mobility of sediment characterize the efficiency of spawning restoration projects, in addition to traditional habitat variables such as water depth, velocity, and grain size. In practice, the resilience of spawning ground restoration tends to be short-lived, as these habitats are typically exposed to regular annual or sub-annual floods (Merz, Pasternack, and Wheaton 2006) and long-term surveys have revealed poor benefit for fish (Thompson 2006). Pulg et al. (2022) highlighted that, across eight study sites, the median spawning area decreased by 26% after 10–18 years, largely due to gravel erosion in regulated rivers. Mechanical intervention can increase the resilience of artificial spawning grounds. Direct injection (Gaeuman 2014), or reshaping after each hydrological event, can offset the scouring of sediment cover. However, these operations are often costly and depend on available gravel reserves, both of which pose significant challenges to the scaling of spawning restoration projects. Passive methods, which involve placing hydraulic structures such as boulders, rocks, logs, or low-level weirs in the riverbed have been shown to favor sediment deposition (Bunte 2004) and have demonstrated effectiveness (Louhi et al. 2016). Depending on boulder placement, one potential drawback is that spawning gravel may still be susceptible to erosion (Hauer et al. 2020).

All of the above methods require a high level of expertise in designing appropriate hydraulic structures. Once defined, such designs may not be transferable to other reaches or rivers, due to their strong dependency on local hydraulic conditions. Understanding key physical mechanisms, along with accurate numerical modeling, is therefore essential for effective restoration in variable configurations. Moreover, for rivers starved of long-term sediment supply, the most effective approach to increase the resilience of artificial spawning ground is not to deposit additional sediment upstream, but rather to stabilize the

replenishment at existing sites. Sufficient sediment transport should be ensured over short distances (a few meters per year), to avoid clogging risks and allow fish to construct nests, while minimizing the potential for rapid erosion or diffusion of added material during floods (Peeters et al. 2021).

Two-dimensional hydraulic models have been widely used to assess habitat characteristics in natural river reaches (Dudley et al. 2022; Grantham 2013), downstream of dams (Bürgler et al. 2023), and in restoration projects (Fischer et al. 2020; Gard 2006; Harrison et al. 2019; Pasternack, Wang, and Merz 2004). Laboratory experiments and hydraulic models coupled with sediment transport modules enable investigation into the spatiotemporal evolution of restoration projects (Battisacco, Franca, and Schleiss 2016; Juez et al. 2016). Combining both approaches could greatly enhance the assessment of the effectiveness and resilience of gravel augmentation projects. It could also be a convenient tool for investigating the effect of boulder arrangement on the stability of spawning grounds and for optimizing their design. As underlined by Hauer et al. (2020), such engineering tools need to be validated.

This study focuses on spawning ground stabilization in a river with a severely limited supply of sediment: the Dordogne River in France. The approach combines field observations, small-scale laboratory experiments, and numerical simulations. The primary objective of this study was to explore the capacity of numerical modeling to reproduce the stabilization of spawning grounds based on a laboratory experiments. The second objective was to assess the potential of boulders to enhance the resilience of artificial spawning grounds. The paper first presents the field site, the experimental setup, and the numerical model. The three approaches are then compared, and prospective numerical scenarios are studied, followed by a discussion on the complementarity of the integrated field-flume-numerical strategy.

2 | Materials and Methods

2.1 | Study Site

The present study was designed to describe the restoration of Salmonid spawning sites in the Dordogne River. The following briefly describes the field application. To create effective spawning grounds for Salmonid species, gravel was replenished at multiple sites along the Dordogne in 2020 and 2022. The work was conducted by EPIDOR (EPTB Dordogne). Boulders were placed transversely in the replenishment areas, resembling a low weir. The boulder arrangement was empirically decided and still required engineering feedback to optimize replenishment resilience.

The spawning site of particular interest to this study is located 45°44.09" N, 1°56'3.14" E, near the town of Argentat, 4.3 km downstream from the Sablier dam operated by EDF (Electricité de France), where loss of small-sized gravel was clearly identified. The width of this river section is about 80–100 m. The average slope is 0.3% and the mean discharge is 100 m³/s. Most of the remaining sediments that compose the river bed are around 20 cm in diameter and are not transported by mean annual flood events.

For the purpose of Salmonid spawning habitats, the replenished sediment diameters range between 2 and 8 cm. The artificial spawning replenishments sediments were deposited along one bank of the river, in an area 15 m wide and between 40 and 80 m long, depending on the site (Figure 1). The replenishment thickness of 35 cm corresponds to the water depth at a low-flow discharge of 30 m³/s. At discharges above this level, the deposit becomes submerged and can be mobilized at higher flow rates. The mobilization of replenished gravel depends on hydraulic events largely controlled by the management of upstream dams within the catchment. At this stage, the complex evolution of hydraulic events is beyond the scope of this paper. However, for laboratory-scale reference, it should be noted that, due to flood control by dams, the maximum flow discharge since the mid-1990s has been around 560 m³/s, corresponding to a biannual flood under natural hydrological conditions and resulting in a water depth of approximately 2.5 m above the replenishment area.

Typical length scales of the boulders used on these sites are around 50 cm. Boulders are densely aligned to touch each other and are arranged in single rows perpendicular to the bank across the entire width of the replenishment area. Two rows of boulders were placed, one downstream and the other mid-length of the 80 m long replenishment area. Field data are scarce and limited to two topographic surveys of the replenishment area conducted before and after a 445 m³/s flood that occurred on February 1, 2021.

2.2 | Experimental Setup

An experimental model was developed at IMFT (Toulouse Institute of Fluid Mechanics) to reproduce the hydro-sedimentary

dynamics of a representative section of the Dordogne spawning site.

Complete similitude between field and laboratory conditions cannot be achieved for such complex systems (El Kadi Abderrezzak et al. 2014). In this study, the choice was made to impose a Froude similarity for the hydraulic regime along with a Shields similarity for the sediment transport regime. This approach preserves the replenishment bed shape between field and laboratory, preventing the formation of ripples or other dune shapes. For the purpose of this research, the Froude number, Fr , and Shields number, θ , are defined as follows:

$$Fr = \frac{q}{g^{1/2}h^{3/2}} \quad (1)$$

$$\theta = \frac{\tau_b}{(\rho_s - \rho_f)gd} \quad (2)$$

with $q = Q/W$ the water discharge per unit width, Q being the discharge, g the gravity, h the water depth, d the grain diameter, ρ_s the grain density, ρ_f the fluid density, and τ_b the basal friction; that is, the fluid shear stress component at the bottom. In the following model, the fluid shear stress at the bottom is written as $\tau_b = f\rho_f q^2 / 8h^2$ with f a turbulent friction factor imposed by the rough bottom, and q/h the mean streamwise velocity. The model for the Shields number is defined as:

$$\theta = \frac{fq^2}{8h^2 \left(\frac{\rho_s}{\rho_f} - 1 \right) gd} \quad (3)$$

In order to satisfy the (Fr, θ) similarity, one considers a simple equilibrium of a 1D flow with the slope, leading to the momentum conservation as $\tau = \rho_f g I h$ (I being the local slope). The



FIGURE 1 | Replenishment for fish spawning in the Dordogne River in 2020. The flow is from right to left. Source: EPIDOR. [Color figure can be viewed at [wileyonlinelibrary.com](https://onlinelibrary.wiley.com)]

system is closed with the Colebrook–White model for the friction factor f :

$$\frac{1}{\sqrt{f}} = -2 \log \left(\frac{\epsilon}{12 Rh} + \frac{2.51}{Re \sqrt{f}} \right) \quad (4)$$

where the friction factor f is related to the roughness scale ϵ , hydraulic radius Rh , and the Reynolds number $Re = q/\nu$, ν being the kinematic viscosity. Since the roughness scale ϵ can be related to the grain diameter of the replenishment d , we assume $\epsilon = d$ here for simplicity and without loss of generality. Finally, using the previous definitions and models, the Froude number and the Shields number can be evaluated for biannual flood events in the field. This yields an estimate of the Froude number ranging from 0.64 to 0.80 and an estimate of the Shields number over the replenishment area between 0.04 and 0.07.

Laboratory experiments were conducted in a straight flume of 7.5 m length, 1 m width, and 50 cm height, resting on a tiltable frame. In all the experimental tests, the longitudinal slope of the flume was fixed at 0.3%, consistent with the river slope. The bottom of the flume was covered with a support made of truncated cone-shaped elements, with a roughness height of 0.7 cm and a diameter of 1.8 cm. At the entrance of the flume, a pump delivered a water flow of $Q = 75$ L/s measured with a flowmeter accurate to about 1 L/s. The water then flowed to the outlet of the flume, which ends in a free fall. To study the mobility of the replenishment, a 2.4 cm-thick gravel deposit was placed in the flume. This replenishment area covered a rectangular surface of 1.67 m length and 50 cm width occupying half the width of the

flume (Figure 2, Case A). The length of the replenishment was scaled to represent a 40 m-long replenishment field site. Its width was not scaled but allows the replenishment gravels to be transported toward the center of the flume, similar to a spanwise dispersion in the field. Replenishment gravel size ranged between 2 and 4 mm, with a median diameter $d = d_{50} = 3.35$ mm. According to the previous similarity analysis with this range of diameters, the laboratory scale led to $Fr = 0.75$ and $\theta = 0.055$. This achieves the expected similitude with field conditions. Although not fully similar, the obtained Reynolds number Re was consistently high enough at both scales to consider the flow fully turbulent.

Non-transportable gravel of complex shape with a typical length of the order of the replenishment thickness, between 2 and 3 cm, mimicking boulders in the field, were placed around the replenishment area according to different configurations (Figure 2, Cases B–J). It should be noted that the term “boulder” is used in this paper independently of the scale considered (flume, model, or field) to refer to “stabilizing material.”

Note that Case B (Figure 2) corresponds to the field arrangement. The placement of these boulders modified the dynamics of the flow above and around the replenishment, as well as grain motion. Various configurations were thus tested to identify which arrangement is most effective in limiting the transport of gravel away from the replenishment area.

During experimental tests, the topographic evolution of the bed was measured with four probes placed transversally above the replenishment deposit (Figure 2, $y = 60, 70, 80$ and 90 cm; $y = 0$ corresponding to the right bank). A rail system enabled

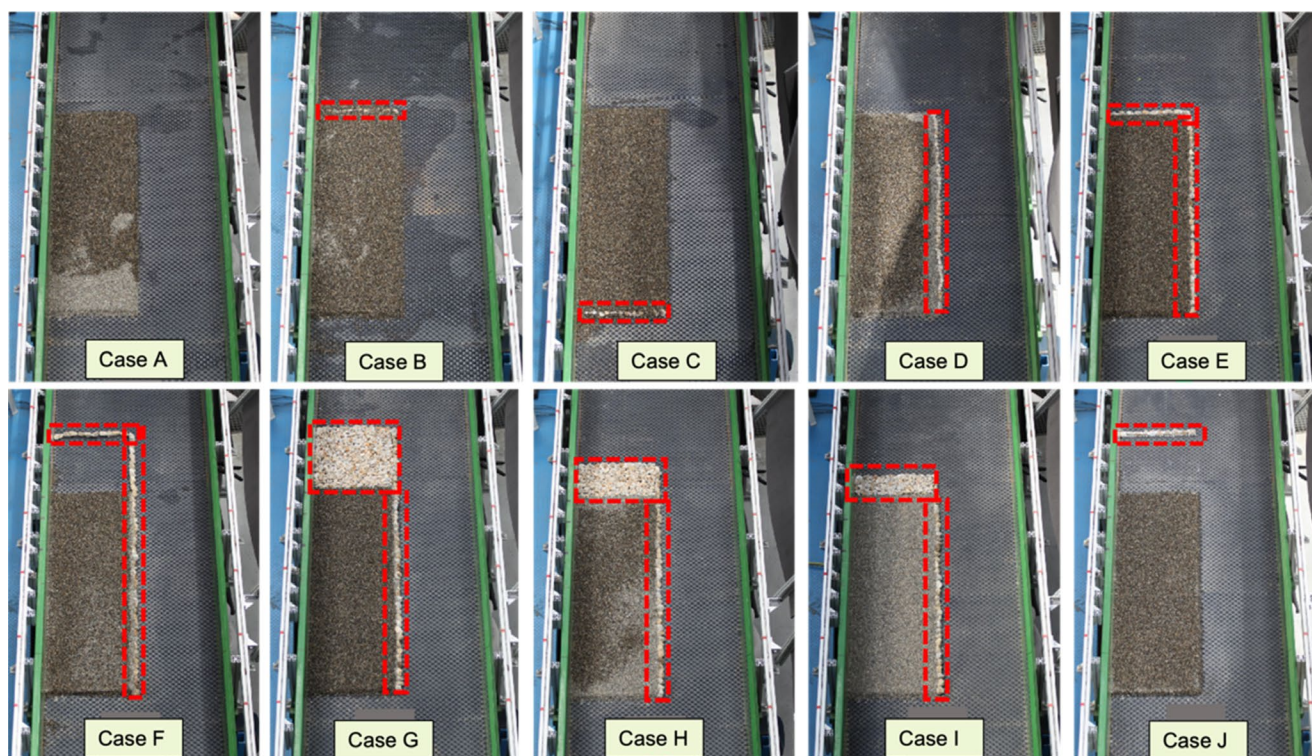


FIGURE 2 | Initial planform configuration of the 10 experimental cases tested at the IMFT lab (Cases A–J). In red: Locations of boulders placed near the gravel replenishment to reduce erosion. The water flows from the lower part to the upper part of the image. [Color figure can be viewed at [wileyonlinelibrary.com](https://onlinelibrary.wiley.com)]

the probes to be moved downstream along the flume. For each probe, 24 measurements were made along the x -axis, which provides the longitudinal topographic profile of the flume and deposit. Data were collected at an interval of 10 min from $t=0$ to $t=40$ min, by stopping the flow and scanning the bed. The experiment ended after 60 min. For each time step, 96 measurements of the flume bottom were taken. A camera was positioned above the flume to capture aerial images tracking the propagation of replenished sediments after 30 and 60 min from the start of each experimental runs.

2.3 | Mathematical and Numerical Modeling System

2.3.1 | Presentation of Numerical and Model Setup

The numerical model is based on the Telemac-Mascaret modeling system, with the hydrodynamic module TELEMAC-2D coupled to the morphodynamic module GAIA (sediment transport and bed evolution; Audouin et al. 2019; Tassi et al. 2023). TELEMAC-2D is based on the solution of the 2D depth-averaged shallow-water equations (SWE) with a closure relationship for the turbulence based on a constant turbulent eddy viscosity, and the Strickler friction law to parameterize roughness effects (Nezu and Nakagawa 1993). GAIA is based on the Exner (1920) equation, where the sediment transport capacity, q_p (m^2/s), is calculated with a bedload capacity formula, relating q_p and fluid flow properties at the top of the sediment surface as local shear stress. Hydrodynamic and morphodynamic modules are coupled at each time step. The equations are discretized on a mesh using the finite-element method (Hervouet 2007).

The computational domain is defined as a rectangle matching the dimensions of the flume. The mesh is irregular and composed of an unstructured network of triangular elements. The size of the elements is variable and depends on the size of the gravel composing the protective wall. The mesh is refined around the replenishment area with an element size of about 0.5 mm instead of 4.6 cm elsewhere (Appendix A.1). The node elevations are calculated with linear interpolation of the topographic data. The model bathymetry corresponds to the elevation of the flume bottom as well as to the thickness of gravel replenishment (2.4 cm). Modeling the rows of non-transportable gravel used in the experiments is complex, as the wall along the replenishment area does not have a constant height. We chose here to model these rows using an impermeable wall of equivalent height corresponding to the minimum size of the experimental gravel, that is, 2 cm.

At the upstream boundary (the inlet of the flume), the flow rate was set at $Q=75$ L/s, that is, equal to the experimental one, while at the downstream boundary (outlet of the flume), the water height was set at the average measured water height in the experimental flume, that is, $h=6.7$ cm. Lateral walls were represented by solid boundaries. The time step was set at 0.002 s, ensuring a Courant Number (CFL) < 0.8 .

At the initial step, three different roughness areas were defined to take into account the diversity of grain sizes in the experiment: the area of the channel covered by fixed truncated cone-shaped

elements (high roughness), the replenishment area (low roughness), and the boulder area with a smaller Strickler coefficient (very high roughness). Roughness varies over time and space as the replenished gravel spreads throughout the flume. Hence, it is assumed that, in the flume, the roughness becomes that of the replenishment as soon as the height of the sediment deposit exceeds 1 cm. Similarly, in the replenishment area, the roughness changes to the value of the flume bottom when the erosion is greater than 1 cm. This threshold value was calibrated to take into account changes in roughness. The riverbed is erodible only where the replenishment area is initially located. The rest of the channel is considered non-erodible, reflecting the laboratory setup.

The roughness is numerically modeled with a Strickler law. The Strickler coefficient (K) of the flume bottom was determined by comparing the longitudinal profile of the simulated and measured water depths. Optimal results were obtained with a Strickler coefficient of $K=35$ $m^{1/3}/s$ for the flume bottom, $K=50$ $m^{1/3}/s$ for the replenishment area, and $K=18$ $m^{1/3}/s$ for the boulder areas (Appendix A.2). A lateral friction with constant roughness is applied to the walls ($K=85$ $m^{1/3}/s$) reflecting the smooth-edge conditions of the experimental flume. Several bedload transport formulas available in GAIA have been tested: Meyer-Peter and Müller (1948), Einstein-Brown (1942/1949), Engelund-Hansen (1967, total sediment transport), Van Rijn (1984), and Wilcock and Crowe (2003). Erosion rates observations in the replenishment area indicated that Van Rijn's formulation is the most suitable for our study (Appendix A.3). This formula is applicable for grain diameter $d=d_{50}=[0.2-2]$ mm. The dimensionless current-induced sediment transport rate is given by:









$$q_{bo} = 0.053 D_* \left(\frac{\theta - \theta_{cr}}{\theta_{cr}} \right)^{2.1} \quad (5)$$

where θ is the Shields number as defined in Equation (2), and θ_{cr} is the critical Shields number equal to 0.047 for the diameter of the replenishment gravels ($D_* = d[(s-1)(g/v^2)]^{1/3} \approx 85$). When the Shields number θ exceeds the critical Shields number, particle motion is initiated. The calculations are performed with a single class of sediment.

2.3.2 | Modeling Strategy

Based on this model implementation and parameterization, a calibration-validation process is performed. First, the model is calibrated on Cases A and G (Figure 2). Case A corresponds to the case of deposit alone, without boulder protection, and Case G corresponds to the configuration with the largest boulder area ratio (Table 1). Case A is used as a reference to evaluate the capacity of the flow to erode and disperse the replenishment. Case G corresponds to the case of a replenishment area surrounded by protective boulders placed along the longitudinal axis of the replenishment, as well as downstream of the replenishment, on a length corresponding to 1/3 of the length of the replenishment, that is, 55 cm (Table 1). It is assumed that Case G corresponds to the maximal protective effort exerted by a river manager. This configuration is used as a reference to evaluate the capacity of

TABLE 1 | Replenishment and spawning ground stabilization configurations.

Case	Replenishment—spawning ground					Stabilization techniques			Boulder area ratio
	Case type	Surface (m ²)	Thickness (m)	Volume (m ³)	Previous replenishment	Initial layout	Lateral boulders (LB)	Perpendicular boulders (PB)	
Initial	Calibration	0		0				No	0
A	Calibration							No	0
B							No	Yes	1.2
C								Yes	4.0
D	Validation	0.835	0.024	0.020	No			No	4.0
E								Yes	5.2
F								Yes (downstream)	6.5
G	Calibration								36.9

(Continues)

TABLE 1 | (Continued)

Case	Case type	Replenishment—spawning ground				Stabilization techniques			
		Surface (m ²)	Thickness (m)	Volume (m ³)	Previous replenishment	Initial layout	Lateral boulders (LB)	Perpendicular boulders (PB)	Boulder area ratio
H									20.5
I	Validation								12.3
J									1.2
M									
N								Tested with and without perpendicular blocks downstream	8.3
O									
T	Prospective scenarios						No		0
U								Tested with and without perpendicular blocks downstream	8.3
Y			Variable ^a	0.0293 ^b	Yes				0
Z			0.036	0.030	No			No	0

^aThe replenishment height ranges between 2.4×10^{-2} and 3.6×10^{-2} m.
^bThis volume corresponds to the sum of the residual material (not eroded during a previous replenishment, 9.34×10^{-3} m³) and a second replenishment (3.0×10^{-2} m³).

the boulders to limit erosion of the replenishment in the model. Calculation results are compared to the topographic evolutions measured in the laboratory by the experimental probes, as well as to the erosion rates measured in situ in the replenishment area. Once the calibration is completed, the numerical model is applied to the other configurations tested in the laboratory, that is, Cases B, C, D, E, F, H, I, and J for validation (Table 1; Appendix A.4). Model accuracy is evaluated with efficiency proxies (Moriassi et al. 2007) based on comparison between numerical results and experimental data (percent bias [PBIAS], RMSE, or root mean standard deviation ratio [RSR]; for details in efficiency proxies, please refer to Appendix A.5).

Prospective scenarios are investigated to evaluate the impact of the shape and distribution of the spawning area on its sustainability (Cases M, N, O, T, U; Table 1). A last couple of scenarios (Y and Z) are investigated to evaluate the role of previous replenishment and replenishment height on the spawning ground dynamic. All prospective scenarios refer to Case I in terms of downstream boulder characteristics (surface, volume and height). It is assumed that these characteristics are well adapted for operational issues. Indeed, a larger volume of boulders would be more difficult for river managers to mobilize and place in the field.

3 | Results

The results are presented in three steps. First, the laboratory experiments are qualitatively compared with the field monitoring to demonstrate the relevance of the chosen similarity. Then, 10 scenarios of boulder arrangement around the replenishment area are studied both experimentally and numerically. The influence of different configurations is compared, a calibration-validation

process is conducted for the numerical model, and the robustness of the simulation is assessed. The validated numerical model is then used as a predictive tool to study seven prospective scenarios corresponding to potential operational cases.

3.1 | Qualitative Comparison of the Experimental Approach With Field Observations

Since the experiment was designed to study the effect of local configuration on the entrainment of a replenishment and the underlying physical mechanisms, the field configuration is not exactly reproduced in experiments. The comparison with the experimental approach is therefore qualitative and based solely on the observed erosion patterns.

The similarity for the small-scale experiment was established a priori for a 5-hour-long biannual flood discharge ($\sim 550 \text{ m}^3/\text{s}$). However, there were important discharge variations in field measurements taken in October 2020 and October 2021. A peak discharge of $445 \text{ m}^3/\text{s}$ recorded over 30 h (with 85 h at discharge levels above $425 \text{ m}^3/\text{s}$ and 190 h above $400 \text{ m}^3/\text{s}$) was lower than the biannual flood discharge. Furthermore, (i) the replenishment in the field represents a repetition of twice the replenishment pattern B (Figure 2 and Figure 3), and (ii) its lateral extent represents a fifth of the river width in the field and half the flume width in the experiment. Accordingly, Case B at the laboratory scale mimics half of the length of the replenishment site in the field. Therefore, a qualitative comparison between laboratory experiments of Case B and the first half of the replenishment site in the field (right side of the replenishment in Figure 3) is relevant. Focusing on the erosion upstream of the first row of boulders, the erosion patterns obtained are very similar in the field and in the experiments (Figure 3).

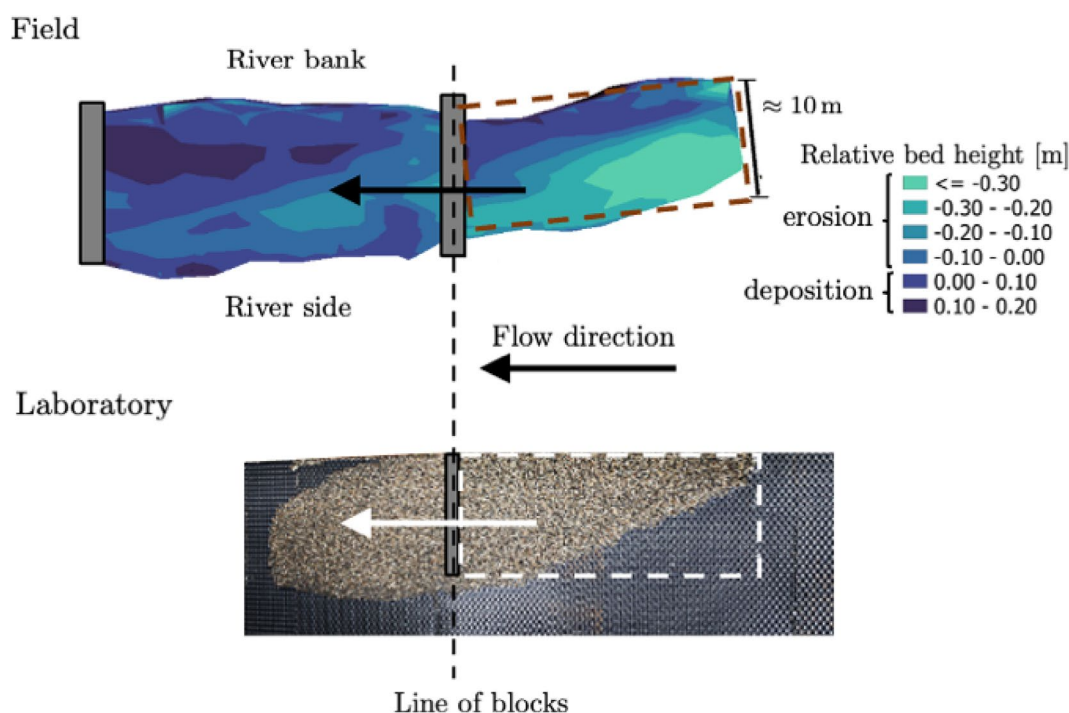


FIGURE 3 | Qualitative comparison between field and laboratory replenishment planform evolution. Dashed lines show the initial position of the replenishment prior to being eroded and transported. [Color figure can be viewed at [wileyonlinelibrary.com](https://onlinelibrary.wiley.com)]

Specifically, on the river side at the most upstream corner (bottom right in Figure 3), erosion in the field is on the order of magnitude of the replenishment thickness (~35 cm), suggesting that the replenishment had been completely eroded in this area, consistent with the experimental observation. As a consequence, a gravel bed pattern emerges downstream of the perpendicular boulders, while a slight diffusion toward the center of the flume is also observed. This is also consistent with the field observation. In particular, the riverside area shows an increase in bed elevation in the field, suggesting a lateral diffusion of the replenishment. Such lateral diffusion was also observed in the laboratory. In addition, erosion downstream of the perpendicular boulders observed in the field was limited compared to that observed upstream, due to the sediment input coming from the replenishment erosion occurring upstream. This is consistent with the emergence of the gravel bed pattern downstream of the boulders observed in the laboratory.

Overall, the replenishment erosion pattern obtained in the experiment was found to be similar to that observed in the field, which allows us to proceed with the use of experiments and numerical modeling.

3.2 | Numerical Calibration-Validation Process Based on Experimental Observations

The numerical model is calibrated by considering two replenishment configurations studied experimentally: simple replenishment without constraining boulders (Case A in Figure 2) and replenishment with a row of boulders on the side and a patch of boulders downstream (Case G in Figure 2). When considering the longitudinal transect at different times ($t=0, 10, 20, 30, 40$ min) and at a given position above the replenishment ($y=0.7$ m, probe 3), the simulated results exhibit a good consistency with the experimental measurements at global scale for both Cases A and G (Figure 4).

For probes 1 and 2 located closer to the sidewalls, both PBIAS and RSR criteria are satisfactory for all time steps (details in Appendix A.5). On the other hand, for probes 3 and 4 located closer to the middle of the flume, the PBIAS criterion degrades over time for Case A, while for Case G, performance remains constant regardless of the time step. This indicates that the numerical model does not fully reproduce the lateral dispersion. Indeed, in Case G, the lateral boulder prevents most of this lateral spread, while in Case A (without any row of boulders) the sediments propagate toward the center of the flume. Therefore, the simulation overestimates the thickness of the sediment wave at $y=0.7$ m in this case. However, according to the RSR criterion which normalizes the mean square error with the standard deviation, the model's performance is considered very good across all time steps and for all probes ($RSR=0.186$).

Common trends can be extracted from both the experiments and the numerical simulations. In Case G, for both experiments and simulations, comparisons of bottom profiles show that, in this configuration, the deposit is less eroded than in Case A (as shown in Figure 4). The simulation results show that the hydrodynamics in the replenishment area are modified by the presence of the perpendicular boulders (Figure 5), consistent with experimental

measurements (not shown here). In addition, the presence of the replenishment alone (i.e., Case A) also impacts the hydrodynamics, since flow acceleration is observed above the replenishment area in the simulation. Specifically, the flow acceleration is reduced by the presence of boulders downstream of the replenishment area. The presence of boulders leads to a decrease in flow velocity and an increase in water height, which subsequently reduces the bottom shear stresses in the whole flume, except above the LB (Appendix A.6). The sediment flow is therefore reduced, and the replenished gravel stays longer at the initial location in Case G (Appendix A.6). Moreover, the model shows a strong replicability of the erosion rate in the spawning ground for both Cases A and G ($RMSE < 3\%$, $PBIAS < 5\%$, and $RSR < 0.5$; Table 2). Consequently, the numerical model is considered calibrated.

Calibrated parameters of Cases A and G (Appendix A.4) have been used in other cases to validate the model. As shown in Figure 6 and Table 2, model performance varies between configurations. More particularly, for Cases H and I where the perpendicular boulder is directly downstream of the gravel replenishment, the model underestimates the observed erosion rate. On the other hand, for Cases F and J, where the perpendicular boulder was placed farther downstream of the replenishment area, little discrepancy is observed between experimental observation and numerical simulation; especially in Case J, there is no lateral boulder to prevent lateral propagation. Specifically, the simulated results diverge only slightly from the measurements ($RMSE$ equal to 6.7%). Similar to Case 1, these results suggest that lateral propagation is not fully captured by the numerical model. Therefore, for Cases E and F, which include lateral boulders, the performance of the numerical model is very good (1.3% deviation for Case E and 3.9% deviation for Case F).

According to the numerical results, the model performs well in reproducing the quantitative and qualitative impacts of the different spawning ground stabilization configurations tested. The model is thus considered as validated and can be further used as a predictive tool under the given configuration.

3.3 | Prospective Numerical Scenarios

First, the lateral distribution of gravel across the width of the river is investigated (Appendix A.7). Comparison of Scenarios A, M, N, and O without stabilization techniques (Figure 7a) shows that a greater lateral spread of the replenishment area results in increased erosion. For example, in Case O where the replenishment area occupies the whole flume width, the erosion rate after 60 min is 74.3%, whereas in Case M, where the replenishment wide is only 25 cm wide (i.e., a quarter of the flume width) and is placed close to the edges of the wall, the erosion rate after 60 min decreases to 47.8%. This result can be explained by higher flow velocities in the center of the flume, owing to the friction of the side walls, which implies higher shear stress and consequent gravel erosion in Scenario O.

Scenario T (Table 1) is designed to provide a better understanding of the effect of dividing the replenishment into two areas, compared to Scenario O. In Scenario T, the replenishment area is divided into two parts: one upstream and the other downstream. The erosion rate at $t=60$ min is lower when the

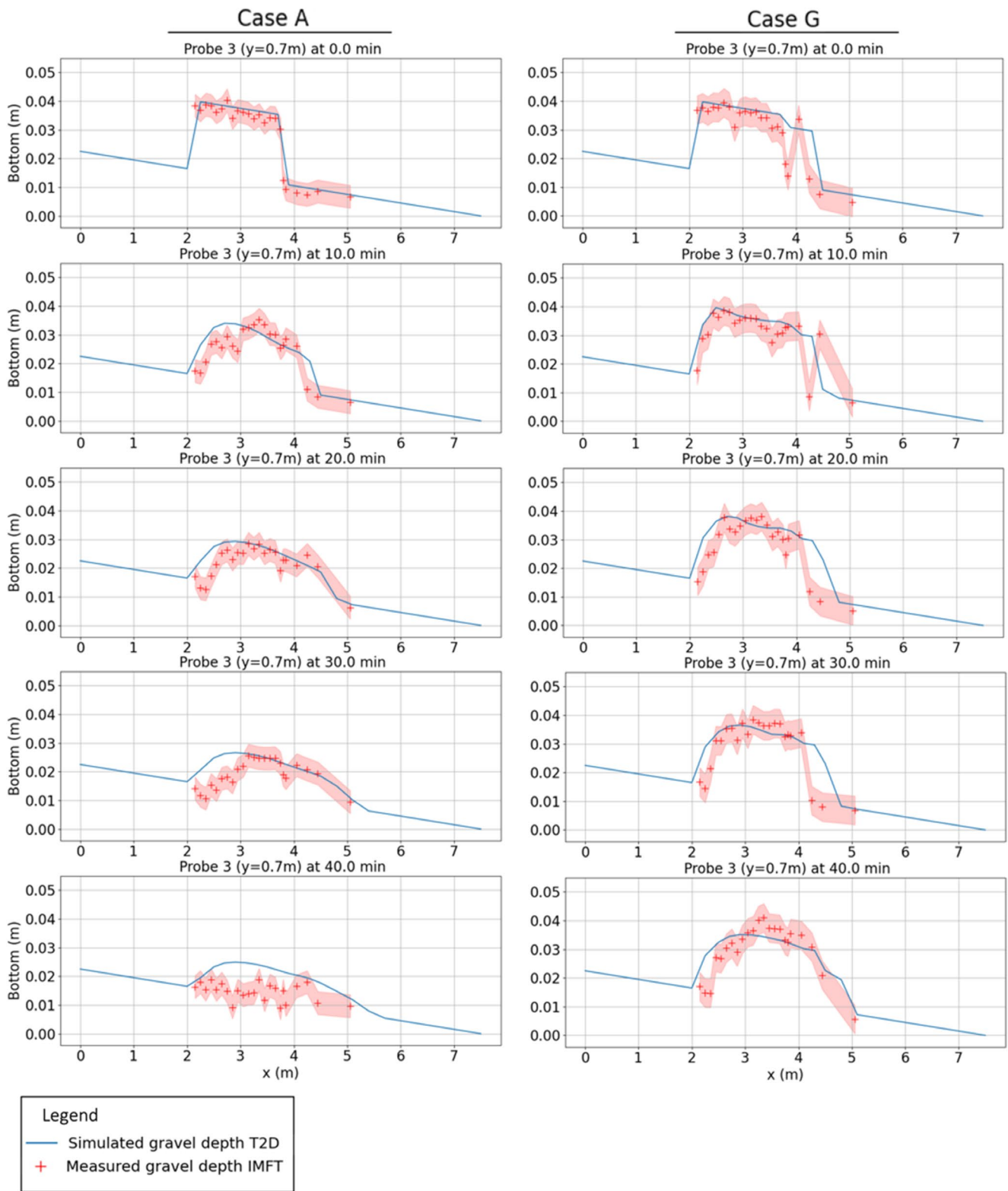


FIGURE 4 | Comparison of the evolution of simulated longitudinal topographic profiles with the measurements of probe 3 ($y=0.70\text{ m}$) for the times $t=0, 10, 20, 30,$ and 40 min after the calibration process in Cases A and G. [Color figure can be viewed at [wileyonlinelibrary.com](https://onlinelibrary.wiley.com)]

replenishment area is divided into two sections (Figure 7b). This can be attributed to modifications in the hydrodynamics above the upstream replenishment area, generated by the backwater effect induced by the downstream replenishment. The downstream replenishment area slows the upstream flow, leading to a reduction in shear stress in the upstream replenishment zone.

It is noteworthy that the erosion rate remains nearly constant between 10 and 20 min, a time interval corresponding to the arrival of sediment eroded from the upstream replenishment area.

The same configurations were tested with the presence of a volume V_b of perpendicular boulders. The presence of perpendicular

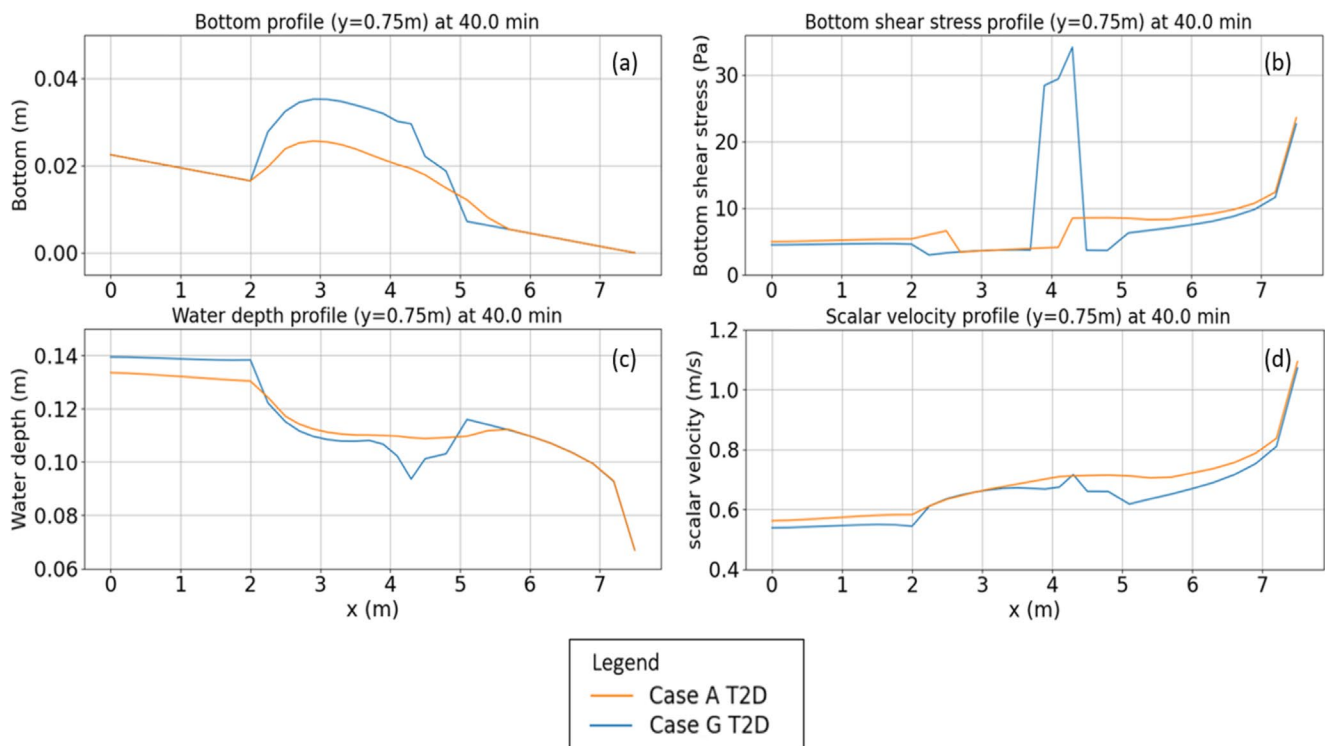


FIGURE 5 | Comparison of simulated variables between Cases A and G: longitudinal profile of flume bottom (a), bottom shear stress (b), water depth (c), and scalar velocity (d) in the middle of the replenishment ($y=0.75\text{m}$), and $t=40\text{min}$. [Color figure can be viewed at [wileyonlinelibrary.com](https://onlinelibrary.wiley.com)]

TABLE 2 | Model evaluation statistics (PBIAS, RMSE, RSR) for the calibration cases (A and G) and the validation cases (B, C, D, E, F, H, I and J).

Cases	PBIAS (%)	RMSE (%)	RSR
A	-3.56	2.61	0.055
G	-0.81	1.39	0.087
B	8.61	3.29	0.072
C	-4.14	3.91	0.091
D	-18.79	7.83	0.165
E	0.61	1.32	0.031
F	12.14	3.87	0.096
H	22.96	3.60	0.127
I	39.29	7.11	0.19
J	22.09	6.68	0.14
Mean value	7.84	4.16	0.11

Note: The calculation is based on the measured erosion rates.

boulders reduces erosion in the replenishment area by approximately 11% for Cases A, N, O, and U and by 7% for Case M.

Boulder arrangement around the replenishment area also influences the shape and distance of the sediment wave propagation (Figure 8). A very small amount of sediment infiltrates into the lateral boulders. In Case A, a free lateral sediment propagation is observed over a significant distance, while in Case D, lateral

sediment propagation is constrained by the lateral boulders. On the other hand, the propagation distance in Case D (1.95 m) is greater than in Case A (1.61 m), which can be explained by the lateral row of boulders forcing the flow to accelerate above the replenishment area. Notably, the presence of the perpendicular boulders downstream of the replenishment area reduces the propagation distance. This distance is further reduced by placing some boulders in the middle of the replenishment area (Figure 8b).

Different scenarios are further evaluated for short-term (around 15 min) and long-term efficiency. In the short term, Scenario T emerges as the worst case, with the most significant erosion. In the very long term (beyond 60 min), it is worth investigating whether Scenario M and Scenario A converge with Scenario N, and if so, what determines the timeframe for such convergence (Figure 7a).

In Scenario Y, the erosion rate is higher than in Case A. This is because the newly replenished gravel ($2.0 \times 10^{-2} \text{m}^3$), placed on top of the previous replenishment ($9.3 \times 10^{-3} \text{m}^3$), creates a thicker deposit than in Case A. This result shows that the initial thickness of the deposit influences the erosion rate of the replenishment (Figure 7c): the greater the initial thickness of the deposit, the greater the flow velocity over the deposit, which increases the local shear stress exerted on the replenished sediment.

The results for Case Z show that the initial thickness of the sediment deposit impacts the erosion rate: the greater the initial thickness, the higher the erosion rate for a similar volume. Furthermore, a comparison of the erosion rates in Scenarios Y

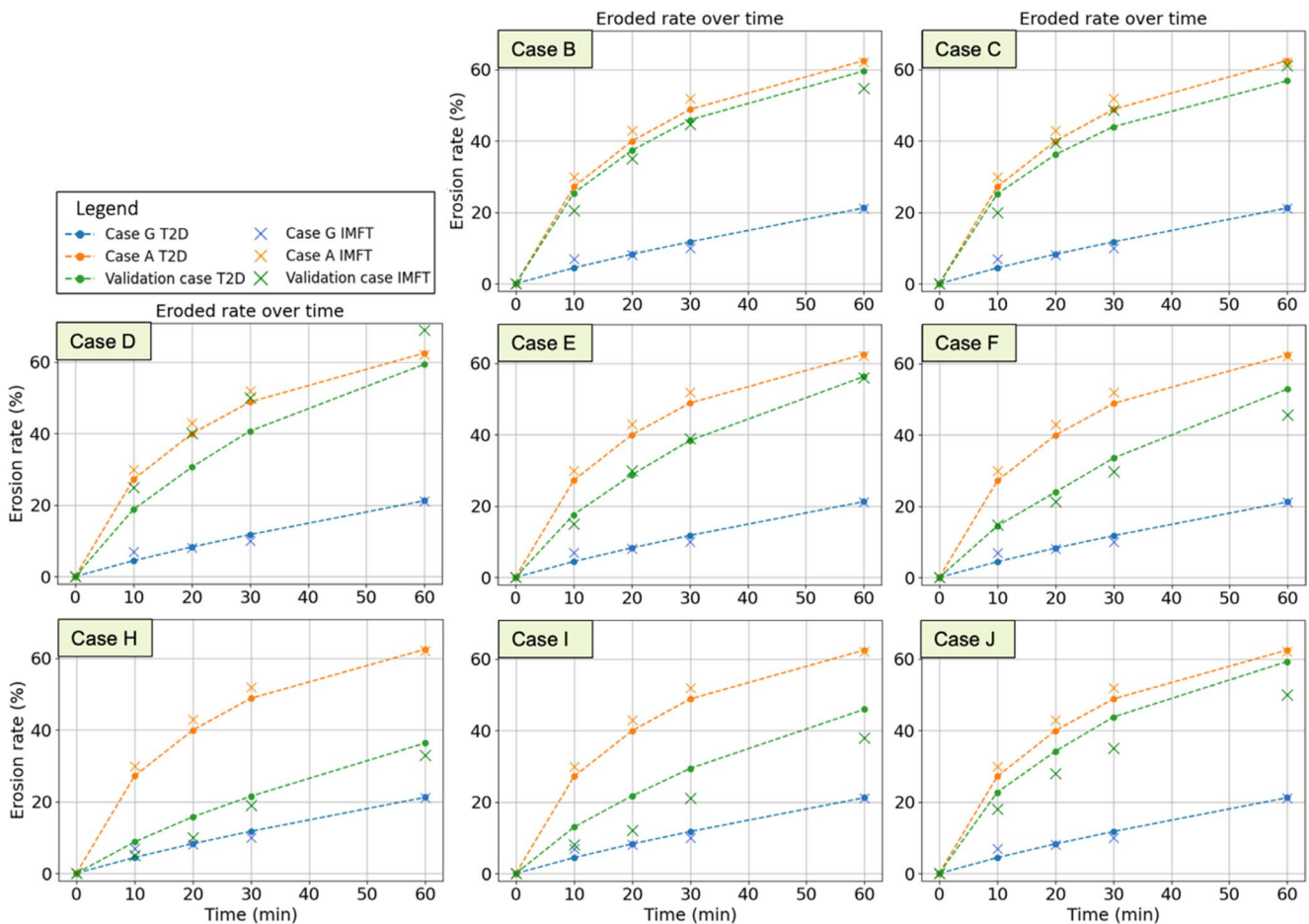


FIGURE 6 | Comparison of the evolution of the simulated and measured erosion rate for the calibration cases (A and G: orange and blue curves, respectively, identical on all graphs) and the validation cases (B–F and H–J: green curves). [Color figure can be viewed at [wileyonlinelibrary.com](https://onlinelibrary.wiley.com)]

and Z shows that the presence of gravel downstream of the first deposit reduces the erosion rate.

4 | Discussion

The integrated field-flume-numerical strategy used in this study offers a robust and efficient approach to investigate the design of in situ fish spawning grounds (Figure 9).

4.1 | From the Field to the Flume

The field observations allow us to define a prototype strategy for spawning ground restoration. This step consists in understanding the physical processes and defining the design pathway for efficient replenishment. Early feedback from the field is useful for go-no-go complementary analyses. Here, the field observations showed that a downstream low weir of boulders could stabilize a spawning ground.

Flume experimental analyses confirmed and assessed a limited number of replenishment stabilization configurations with frontal and lateral rows of boulders. Thanks to real-time measurements and observations on a very fine spatiotemporal scale, the hydromorphological processes can be readily evaluated in detail during the flume experiment. The main inconveniences

in simulation relate to limitations in cost, human resources and time, as well as laboratory restrictions. Compared to a complex river channel, the experimental setup is very simple: it is straight, without any slope break, and of constant width. Notwithstanding this simplicity, the physical model allowed us to investigate in detail the effects of the row of boulders, and to explain the relevant physical processes occurring in the field. With the slope and discharge ranges considered in the present study, the length of the flume does not allow the flow to be strictly uniform over the whole sediment patch. If these differences were large, they could have biased the experimental comparisons of the configurations, but in fact they are very limited. To evaluate this limitation, a simulation comparing the erosion of the same patch of sediment located at 1.147 and 2.147 m from the downstream end of the flume was conducted and the differences of sediment transport between the two cases were found to be very small (Appendix A.7). This limitation therefore does not impact the comparison between field and experimental observation, as the flume flow is well simulated.

4.2 | From the Flume to the Numerical Model

The numerical model calibrated and validated on the flume experiments allowed us to enlarge configurations of replenishment stabilization, and to underline the main control factors of the replenishment evolution over time and space. First, the

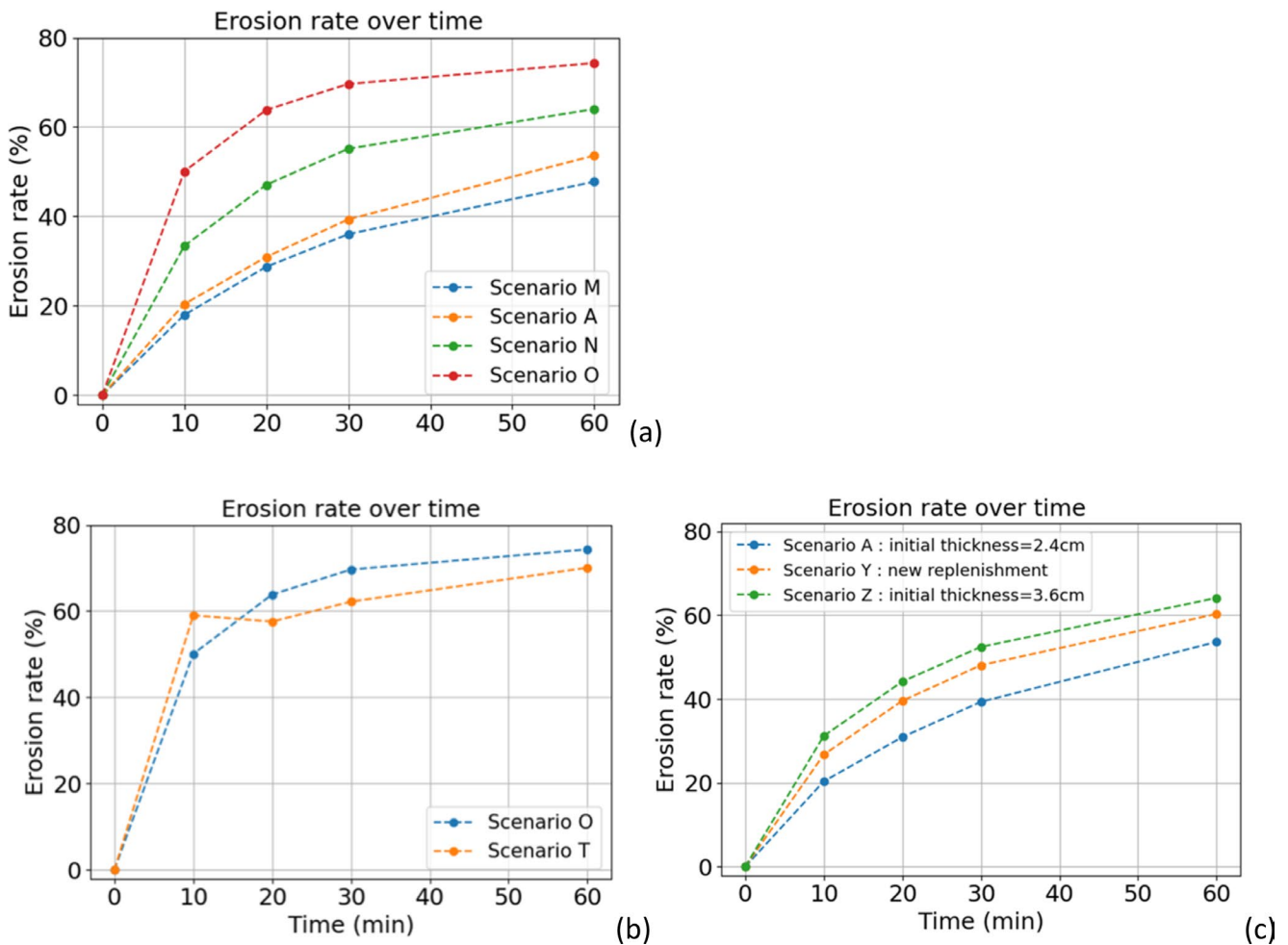


FIGURE 7 | Comparison of erosion rate over time for prospective scenarios: (a) the effects of varying lateral extent of sediment deposit (Scenarios A, M, N, and O); (b) the effects of dividing the replenishment into two zones with one downstream of the other (Scenarios O and T); (c) the effects of varying initial sediment replenishment thickness (Scenarios A, Y, and Z). [Color figure can be viewed at [wileyonlinelibrary.com](https://onlinelibrary.wiley.com)]

comparison between experimental and numerical bed evolutions confirmed the relevance of the numerical tool to satisfactorily reproduce physical processes. In particular, both the shape of the erosion pattern and the quantitative estimation of the eroded volume were well captured by the numerical model. This shows the ability of a depth-averaged approach to capture the main processes of erosion, even for sharp roughness transitions (replenishment gravel, boulders, and flume bed), according to a relatively small number of numerical parameters (Appendix A.4).

A reliable numerical model involves calibrating the friction coefficient and comparing with the observed bed evolution. These steps are supported by data which can be monitored in the laboratory. The row of boulders (lateral or front low wall/weir) was simulated by integrating their elevation in the Digital Elevation Model and using an adequate friction coefficient, in which boulders were assumed to be stable. This proved to be an efficient way of simulating their effect on hydraulic and sediment transport. There was no need to include local and small-scale flow disturbance around the boulders which could have been simulated only with CFD (computational fluid dynamics) approaches (Liu et al. 2017). While experiments show that a small amount of sediment infiltrates the row of boulders, the chosen boulder

simulation does not allow us to simulate this effect. However, it appears to be negligible for simulating the stabilization and the propagation of the spawning ground. Overall, the comparison between experimental and numerical bed evolutions confirmed the relevance of the numerical tool and associated strategy for modeling boulders to satisfactorily reproduce physical processes of erosion.

4.3 | Guidelines From Laboratory and Numerical Results to the Field

The combination of hydraulic and sediment numerical models proved adequate for robust testing of a large range of configurations. This part of the study aims to establish the suitability of the method as a benchmark tool for predicting the evolution of in situ spawning grounds.

As mentioned above, a reliable numerical model involves calibrating the friction coefficient and comparing with the observed bed evolution. The use of such an approach in the field would require the acquisition of flow measurements. For example, 2D flow fields with Large Scale Particle Image Velocimetry (Fujita, Muste, and Kruger 1998) would be recommended for calibrating

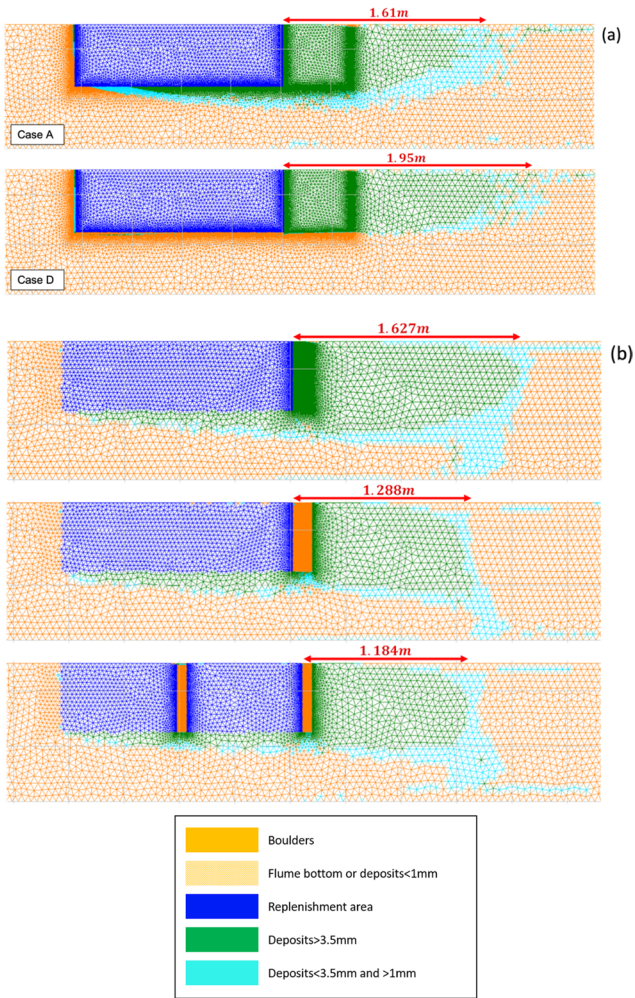


FIGURE 8 | Comparison of the shape of the sediment spread for Scenarios A and D (a) and comparison of the distance of the sediment spread for Scenario A depending on the presence and the distribution of protective boulders (b). [Color figure can be viewed at [wileyonlinelibrary.com](https://onlinelibrary.wiley.com)]

the friction coefficient over a large area, including different roughness surfaces. Monitoring of water elevation at several locations would also yield information relevant to the roughness coefficient. High-resolution bathymetric data before and after replenishment would allow good evaluation of bed evolution. Passive Integrated Transponder (PIT) tagging of scour chains would provide supplementary insight into bed evolution (Hassan 1990; Lamarre, MacVicar, and Roy 2005). These measurements and topographic changes would help to validate the modeled morphological evolution; for example, it would define the most suitable formula for transport capacity. Such a model would be used to design a stable spawning ground prior to gravel augmentation. However, it may be difficult to obtain bed evolution data in the field. Therefore, it is crucial to monitor hydraulic data at different discharge stages. The difficulty of obtaining such data from field measurements highlights the importance of using the experimental approach, with its more readily accessible monitoring.

Several similarities were observed with experimental methods of stockpiling where gravel were not submerged. Firstly, a replenishment deposit with only limited transverse occupation of a flume erodes less quickly than a replenishment occupying the whole width, as already observed by Friedl, Weitbrecht, and Boes (2018). Secondly, when the replenishment is divided into two areas upstream and downstream of each other, the downstream replenishment limits gravel erosion of the upstream replenishment, as found in previous studies by Battisacco, Franca, and Schleiss (2016). Finally, during a subsequent gravel replenishment, the presence of the sediment from the previous replenishment in the flume further limits the erosion, as shown by Bösch et al. (2016). Finally, we confirm that replenishment width and height are of utmost importance to the design of spawning restoration.

The tested prospective scenarios offer guidance on how to stabilize spawning grounds with boulders in actual rivers. Hauer et al. (2020) pointed out how the presence of boulders can have

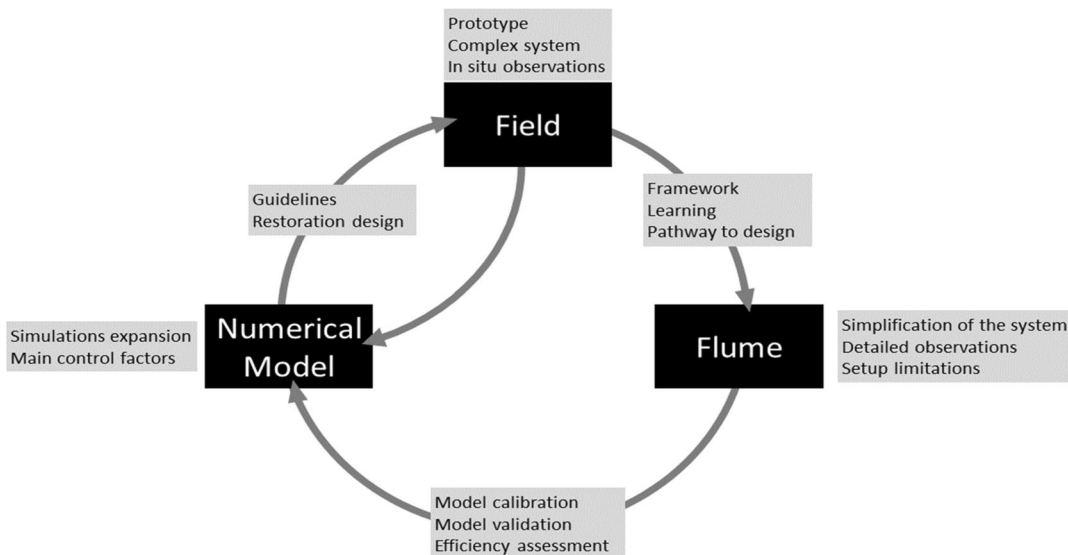


FIGURE 9 | The integrated field-flume-numerical approach to design in situ fish spawning habitats. [Color figure can be viewed at [wileyonlinelibrary.com](https://onlinelibrary.wiley.com)]

unwanted side-effects, depending on how they are placed. While boulders can prevent the erosion of spawning gravel, they may also increase its movement. Cross-validation of experimental and numerical models support the use of a row of boulders for stabilization. The numerical model provides a convenient tool for adapting the design of the row to the in situ context. Varying discharges can be numerically tested in order to assess design resilience, that is, which flood gravel will be transported downstream. Boulder height may also play a role in slowing the flow over the gravel replenishment. However, these boulders should not interrupt sediment transport if they span the entire width of the river. Moreover, it is also necessary to consider that greater acceleration downstream of excessively high boulders can intensify flow inertia and cause erosion downstream.

Compared to a complex river channel the experimental setup is quite simple. The flume was straight, without any slope break, and of constant width. While it allows us to investigate the specific effect of the row of boulders, more complex geometry is required to predict details of the replenishment evolution in the field. As two-dimensional horizontal (2DH) modeling of sediment transport was previously validated in rivers (Brousse et al. 2022; Li et al. 2023), it is, in the present study, the first a priori step before using this approach in natural rivers. This study, therefore, is a proof of concept before using 2D sediment and hydraulics in rivers to design augmentation work. These results encourage the use of 2D hydromorphological modeling to predict the stability of artificial spawning grounds in the field.

In some rivers, suspended fine sediment can clog the spawning ground (Dubuis and De Cesare 2023), reducing gravel movement that can adversely affect spawning (Peeters et al. 2021). These authors observed that a travel distance of 3 m/year for gravel sustains the spawning area. In the Dordogne River, the amount of fine sediment is very low and unlikely to affect the artificial spawning ground. If de-clogging were ever needed, it would be easier to rework the replenishment area than to import new sediment.

In any event, it is essential to analyze in situ observations, not only to validate the numerical modeling, but also to refine design recommendations for boulder placement. For example, on the Dordogne River, there is a lack of complete bathymetric data to enable simulation of the whole reach.

5 | Conclusion and Perspectives

The resilience of artificial spawning grounds in sediment-starved rivers is studied in terms of use of boulders to stabilize gravel replenishment. The objective of the integrated field-flume-numerical strategy was to preserve conditions for fish reproduction by limiting the transport of replenished material. Design optimization is evaluated based on the integrated framework combining an experimental setup and numerical modeling.

The study demonstrated that the resilience of spawning restoration is improved by using transversal or longitudinal rows of boulders around the replenishment. The numerical model built with TELEMAC2D and GAIA solvers accurately reproduced the flow dynamics, sediment transport, and morphodynamics of

the river/flume, showing correct simulation of erosion rates and sediment propagation compared to the flume data. Specifically, the model effectively simulated the bed evolution in the replenishment area.

The primary factor controlling stabilization is the quantity and configuration of boulders. A significant number of boulders downstream of the replenishment area altered the flow dynamics above the spawning ground, slowing down the flow and reducing shear stress. This configuration aids river managers in optimizing stabilization design. A limited number of boulders placed along the longitudinal axis and downstream of the replenishment, acting as a low weir, provided a good compromise between cost and stabilization efficacy.

When the boulder configuration is limited or determined by field conditions, prospective scenarios illustrated that the shape and distribution of the replenishment deposit significantly impact its resilience. A replenishment deposit with a limited transverse occupation eroded less quickly than one occupying the full width of the flume section. Replenishment resilience could also be enhanced by dividing the replenishment into two areas, upstream and downstream of each other.

In future research, the experimental setup and the numerical model can be used to investigate the effects of the transverse and longitudinal bed slopes. The validated numerical model will also provide insights into the longer-term evolution of the replenished area and the effect of variable discharges. Other prospective scenarios of boulder distributions downstream of the replenishment area can be studied. Different kinds of artificial structures can be tried out such as weirs made of wood (Peeters et al. 2021) may be effective for gravel stabilization. Their impact on the upstream backwater could be tested in an experimental setup, in situ or with the use of numerical models (Addy and Wilkinson 2019). Two-dimensional sediment and hydraulic modeling can be coupled with habitat modeling (Von Gunten, Le Coarer, and Zaoui 2018) to assess the improvement in fish habitats. Moreover, gravel augmentation of a spawning ground may be combined with an upstream stockpile in the case of rivers where high mobility of gravel is foreseen. An upstream reserve of sediments may replace the eroded gravel from the spawning area. Modeling tools could help to design the location of this sediment reserve. The conclusions of this work could also be complemented with future feedback from the field, particularly from operations conducted on the Dordogne River.

Acknowledgments

The authors acknowledge the partial support of the ANR project 15-CE01-0013 SEDIFLO: "Modelling and simulation of solid transport in rivers." Furthermore, the authors wish to thank B. Munir for performing the experiments, the EPIDOR for providing field data, and Sébastien Boyaval for fruitful discussions. Special appreciation is extended to Junjian Deng for his thorough review and valuable improvements to the manuscripts.

Data Availability Statement

The data that support the findings of this study are available from the corresponding author upon reasonable request.

References

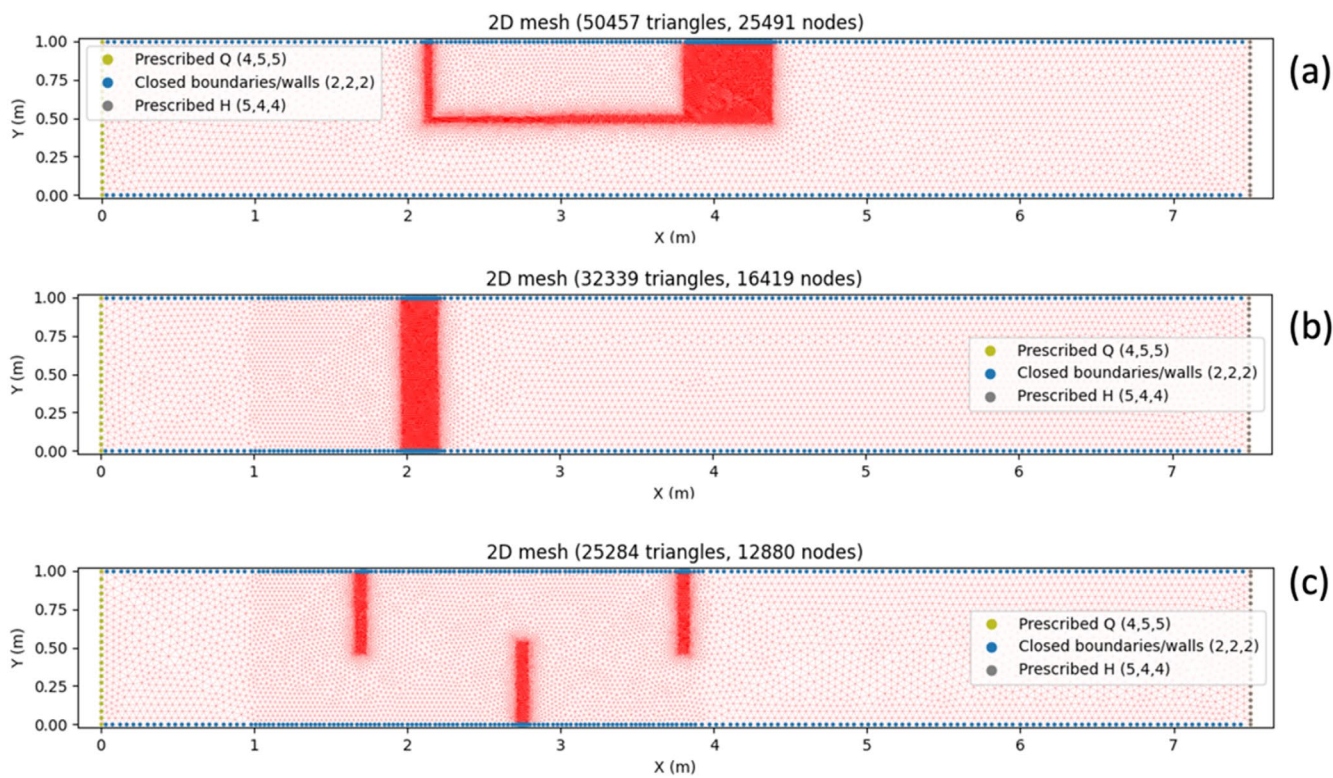
- Addy, S., and M. E. Wilkinson. 2019. "Representing Natural and Artificial In-Channel Large Wood in Numerical Hydraulic and Hydrological Models." *WIREs Water* 6, no. 6: e1389. <https://doi.org/10.1002/wat2.1389>.
- Arnaud, F., H. Piégay, D. Béal, P. Collery, L. Vaudor, and A. J. Rollet. 2017. "Monitoring Gravel Augmentation in a Large Regulated River and Implications for Process-Based Restoration: Monitoring Gravel Augmentation in a Large Regulated River." *Earth Surface Processes and Landforms* 42, no. 13: 2147–2166. <https://doi.org/10.1002/esp.4161>.
- Audouin, Y., T. Benson, M. Delinares, et al. 2019. "Introducing GAIA, The Brand New Sediment Transport Module of the TELEMAC-MASCARET System." In *XXVth TELEMAC-MASCARET User Conference*, Toulouse, October 15–17, 2019. <https://doi.org/10.5281/zenodo.3611600>.
- Battisacco, E., M. J. Franca, and A. J. Schleiss. 2016. "Sediment Replenishment: Influence of the Geometrical Configuration on the Morphological Evolution of Channel-Bed: Sediment Replenishment Volumes and Channel-Bed Morphology." *Water Resources Research* 52, no. 11: 8879–8894. <https://doi.org/10.1002/2016WR019157>.
- Beechie, T. J., M. Liermann, E. M. Beamer, and R. Henderson. 2005. "A Classification of Habitat Types in a Large River and Their Use by Juvenile Salmonids." *Transactions of the American Fisheries Society* 134, no. 3: 717–729. <https://doi.org/10.1577/T04-062.1>.
- Beschta, R. L., and W. S. Platts. 1986. "Morphological Features of Small Streams: Significance and Function." *Journal of the American Water Resources Association* 22, no. 3: 369–379. <https://doi.org/10.1111/j.1752-1688.1986.tb01891.x>.
- Brandt, S. A. 2000. "Classification of Geomorphological Effects Downstream of Dams." *Catena* 40, no. 4: 375–401. [https://doi.org/10.1016/S0341-8162\(00\)00093-X](https://doi.org/10.1016/S0341-8162(00)00093-X).
- Brenna, A., N. Surian, and L. Mao. 2020. "Response of a Gravel – Bed River to Dam Closure: Insights From Sediment Transport Processes and Channel Morphodynamics." *Earth Surface Processes and Landforms* 45, no. 3: 756–770. <https://doi.org/10.1002/esp.4750>.
- Brousse, G., G. Arnaud-Fassetta, F. Liébault, et al. 2020. "Channel Response to Sediment Replenishment in a Large Gravel-Bed River: The Case of the Saint-Sauveur Dam in the Buëch River (Southern Alps, France)." *River Research and Applications* 36, no. 6: 880–893. <https://doi.org/10.1002/rra.3527>.
- Brousse, G., N. Claude, F. Cordier, R. Loire, and M. Jodeau. 2022. "2D Morphodynamic Modelling as a Predictive Tool for Gravel Replenishment: The Saint-Sauveur Dam Case Study." *International Journal of River Basin Management* 22, no. 3: 389–402. <https://doi.org/10.1080/15715124.2022.2153857>.
- Bunte, K. 2004. "State of the Science Review: Gravel Mitigation and Augmentation Below Hydroelectric Dams: A Geomorphological Perspective." Report submitted to the Stream Systems Technology Center, USFDA. <https://doi.org/10.13140/2.1.1094.3361>.
- Bösch, L., E. Battisacco, M. J. Franca, and A. Schleiss. 2016. "Influence of Consecutive Sediment Replenishment on Channel Bed Morphology." In *River Flow 2016. The International Conference on Fluvial Hydraulics (River Flow 2016)*, 1147–1154. St. Louis, USA: CRC Press. <https://doi.org/10.1201/9781315644479-182>.
- Bürgler, M., D. F. Vetsch, R. M. Boes, and D. Vanzo. 2023. "Systematic Comparison of 1D and 2D Hydrodynamic Models for the Assessment of Hydropeaking Alterations." *River Research and Applications* 39, no. 3: 460–477. <https://doi.org/10.1002/rra.4051>.
- Chu, T. W., and A. Shirmohammadi. 2004. "Evaluation of the SWAT Model's Hydrology Component in the Piedmont Physiographic Region of Maryland." *Transactions of the ASAE* 47, no. 4: 1057–1073. <https://doi.org/10.13031/2013.16579>.
- Dubuis, R., and G. De Cesare. 2023. "The Clogging of Riverbeds: A Review of the Physical Processes." *Earth-Science Reviews* 239: 104374. <https://doi.org/10.1016/j.earscirev.2023.104374>.
- Dudley, P. N., S. N. John, M. E. Daniels, and E. M. Danner. 2022. "Using Decades of Spawning Data and Hydraulic Models to Construct a Temperature-Dependent Resource Selection Function for Management of an Endangered Salmonid." *Canadian Journal of Fisheries and Aquatic Sciences* 79, no. 1: 73–81. <https://doi.org/10.1139/cjfas-2021-0022>.
- El Kadi Abderrezzak, K., A. Die Moran, E. Mosselman, J.-P. Bouchard, H. Habersack, and D. Aelbrecht. 2014. "A Physical, Movable-Bed Model for Non-Uniform Sediment Transport, Fluvial Erosion and Bank Failure in Rivers." *Journal of Hydro-Environment Research* 8, no. 2: 95–114. <https://doi.org/10.1016/j.jher.2013.09.004>.
- Exner, F. M. 1920. "Zur Physik der Dünen. Akademie der Wissenschaften Wien." *Mathematisch-Naturwissenschaftliche Klasse* 129, no. 2a: 929–952.
- Fischer, J. L., G. P. Filip, L. K. Alford, E. F. Roseman, and L. Vaccaro. 2020. "Supporting Aquatic Habitat Remediation in the Detroit River Through Numerical Simulation." *Geomorphology* 353: 107001. <https://doi.org/10.1016/j.geomorph.2019.107001>.
- Friedl, F., V. Weitbrecht, and R. M. Boes. 2018. "Erosion Pattern of Artificial Gravel Deposits." *International Journal of Sediment Research* 33, no. 1: 57–67. <https://doi.org/10.1016/j.ijsrc.2017.08.003>.
- Fujita, I., M. Muste, and A. Kruger. 1998. "Large-Scale Particle Image Velocimetry for Flow Analysis in Hydraulic Engineering Applications." *Journal of Hydraulic Research* 36, no. 3: 397–414. <https://doi.org/10.1080/00221689809498626>.
- Gaeuman, D. 2014. "High-Flow Gravel Injection for Constructing Designed In-Channel Features: High-Flow Gravel Injection." *River Research and Applications* 30, no. 6: 685–706. <https://doi.org/10.1002/rra.2662>.
- Gard, M. 2006. "Modeling Changes in Salmon Spawning and Rearing Habitat Associated With River Channel Restoration." *International Journal of River Basin Management* 4, no. 3: 201–211. <https://doi.org/10.1080/15715124.2006.9635289>.
- Geist, D. R., and D. D. Dauble. 1998. "Redd Site Selection and Spawning Habitat Use by Fall Chinook Salmon: The Importance of Geomorphic Features in Large Rivers." *Environmental Management* 22, no. 5: 655–669. <https://doi.org/10.1007/s002679900137>.
- Grantham, T. E. 2013. "Use of Hydraulic Modelling to Assess Passage Flow Connectivity for Salmon in Streams: Hydraulic Modelling of Fish Passage Flows." *River Research and Applications* 29, no. 2: 250–267. <https://doi.org/10.1002/rra.1591>.
- Gupta, H. V., S. Sorooshian, and P. O. Yapo. 1999. "Status of Automatic Calibration for Hydrologic Models: Comparison with Multilevel Expert Calibration." *Journal of Hydrologic Engineering* 4, no. 2: 135–143. [https://doi.org/10.1061/\(ASCE\)1084-0699\(1999\)4:2\(135\)](https://doi.org/10.1061/(ASCE)1084-0699(1999)4:2(135)).
- Harrison, L. R., E. Bray, B. Overstreet, et al. 2019. "Physical Controls on Salmon Redd Site Selection in Restored Reaches of a Regulated, Gravel-Bed River." *Water Resources Research* 55, no. 11: 8942–8966. <https://doi.org/10.1029/2018WR024428>.
- Hassan, M. A. 1990. "Scour, Fill, and Burial Depth of Coarse Material in Gravel Bed Streams." *Earth Surface Processes and Landforms* 15, no. 4: 341–356. <https://doi.org/10.1002/esp.3290150405>.
- Hauer, C., U. Pulg, F. Reisinger, and P. Flödl. 2020. "Evolution of Artificial Spawning Sites for Atlantic Salmon (*Salmo salar*) and Sea Trout (*Salmo trutta*): Field Studies and Numerical Modelling in Aurland, Norway." *Hydrobiologia* 847, no. 4: 1139–1158. <https://doi.org/10.1007/s10750-019-04173-1>.
- Hervouet, J.-M. 2007. *Hydrodynamics of Free Surface Flows: Modelling With the Finite Element Method*. Chichester, UK: John Wiley & Sons, Ltd. <https://doi.org/10.1002/9780470319628>.

- Juez, C., E. Battisacco, A. J. Schleiss, and M. J. Franca. 2016. "Assessment of the Performance of Numerical Modeling in Reproducing a Replenishment of Sediments in a Water-Worked Channel." *Advances in Water Resources* 92: 10–22. <https://doi.org/10.1016/j.advwatres.2016.03.010>.
- Koch, F. G., and C. Flokstra. 1981. Bed Level Computations for Curved Alluvial Channels. Proceedings of the XIXth Congress of the International Association for Hydraulic Research, New Delhi, India. Delft Hydraulics Publication No. 240.
- Kondolf, G. M. 1997. "PROFILE: Hungry Water: Effects of Dams and Gravel Mining on River Channels." *Environmental Management* 21, no. 4: 533–551. <https://doi.org/10.1007/s002679900048>.
- Kondolf, G. M., and M. G. Wolman. 1993. "The Sizes of Salmonid Spawning Gravels." *Water Resources Research* 29, no. 7: 2275–2285. <https://doi.org/10.1029/93WR00402>.
- Kondolf, G. M., Y. Gao, G. W. Annandale, et al. 2014. "Sustainable Sediment Management in Reservoirs and Regulated Rivers: Experiences From Five Continents." *Earth's Futures* 2, no. 5: 256–280. <https://doi.org/10.1002/2013EF000184>.
- Lamarre, H., B. MacVicar, and A. G. Roy. 2005. "Using Passive Integrated Transponder (PIT) Tags to Investigate Sediment Transport in Gravel-Bed Rivers." *Journal of Sedimentary Research* 75, no. 4: 736–741. <https://doi.org/10.2110/jsr.2005.059>.
- Li, J., N. Claude, P. Tassi, F. Cordier, A. Crosato, and S. Rodrigues. 2023. "River Restoration Works Design Based on the Study of Early-Stage Vegetation Development and Alternate Bar Dynamics." *River Research and Applications* 39, no. 9: 1682–1695. <https://doi.org/10.1002/rra.4188>.
- Liu, Y., T. Stoesser, H. Fang, A. Papanicolaou, and A. G. Tsakiris. 2017. "Turbulent Flow Over an Array of Boulders Placed on a Rough, Permeable Bed." *Computers & Fluids* 158: 120–132. <https://doi.org/10.1016/j.compfluid.2017.05.023>.
- Louhi, P., T. Vehanen, A. Huusko, A. Mäki-Petäys, and T. Muotka. 2016. "Long-Term Monitoring Reveals the Success of Salmonid Habitat Restoration." *Canadian Journal of Fisheries and Aquatic Sciences* 73, no. 12: 1733–1741.
- Mendoza, A., J. D. Abad, E. Langendoen, D. Wang, P. Tassi, and K. El Kadi Abderrezzak. 2017. "Effect of Sediment Transport Boundary Conditions on the Numerical Modeling of Bed Morphodynamics." *Journal of Hydraulic Engineering* 143, no. 4: 04016099. [https://doi.org/10.1061/\(ASCE\)HY.1943-7900.0001208](https://doi.org/10.1061/(ASCE)HY.1943-7900.0001208).
- Merz, J. E., G. B. Pasternack, and J. M. Wheaton. 2006. "Sediment Budget for Salmonid Spawning Habitat Rehabilitation in a Regulated River." *Geomorphology* 76, no. 1–2: 207–228. <https://doi.org/10.1016/j.geomorph.2005.11.004>.
- Moriassi, D. N., J. G. Arnold, M. W. Van Liew, R. L. Bingner, R. D. Harmel, and T. L. Veith. 2007. "Model Evaluation Guidelines for Systematic Quantification of Accuracy in Watershed Simulations." *Transactions of the ASABE* 50, no. 3: 885–900. <https://doi.org/10.13031/2013.23153>.
- Mörtl, C., and G. De Cesare. 2021. "Sediment Augmentation for River Rehabilitation and Management—A Review." *Land* 10, no. 12: 1309. <https://doi.org/10.3390/land10121309>.
- Nezu, I., and H. Nakagawa. 1993. *Turbulence in Open-Channel Flows*. Rotterdam: A. A. Balkema (IAHR proceedings).
- Ock, G., T. Sumi, and Y. Takemon. 2013. "Sediment Replenishment to Downstream Reaches Below Dams: Implementation Perspectives." *Hydrological Research Letters* 7, no. 3: 54–59. <https://doi.org/10.3178/hrll.7.54>.
- Pasternack, G. B., C. L. Wang, and J. E. Merz. 2004. "Application of a 2D Hydrodynamic Model to Design of Reach-Scale Spawning Gravel Replenishment on the Mokelumne River, California." *River Research and Applications* 20, no. 2: 205–225. <https://doi.org/10.1002/rra.748>.
- Peeters, A., G. Houbrechts, B. de le Court, E. Hallot, J. van Campenhout, and F. Petit. 2021. "Suitability and Sustainability of Spawning Gravel Placement in Degraded River Reaches, Belgium." *Catena* 201: 105217. <https://doi.org/10.1016/j.catena.2021.105217>.
- Petts, G. E. 1984. *Impounded Rivers: Perspectives for Ecological Management*. Chichester: Wiley. Accessed September 9, 2021. <https://westminsterresearch.westminster.ac.uk/item/94x30/impounded-river-s-perspectives-for-ecological-management>.
- Pulg, U., R. J. Lennox, S. Stranzl, et al. 2022. "Long-Term Effects and Cost-Benefit Analysis of Eight Spawning Gravel Augmentations for Atlantic Salmon and Brown Trout in Norway." *Hydrobiologia* 849, no. 2: 485–507. <https://doi.org/10.1007/s10750-021-04646-2>.
- Roni, P., G. R. Pess, T. J. Beechie, and K. M. Hanson. 2014. Fish-Habitat Relationships and the Effectiveness of Habitat Restoration. U.S. Dept. Commer., NOAA, National Marine Fisheries Service, Northwest Fisheries Science Center, Seattle, WA, USA. NOAA Tech. Memo. NMFS-NWFSC-127. <https://repository.library.noaa.gov/view/noaa/4758>.
- Singh, J., H. V. Knapp, J. G. Arnold, and M. Demissie. 2005. "Hydrological Modeling of the Iroquois River Watershed Using HSPF and SWAT." *Journal of the American Water Resources Association (JAWRA)* 41, no. 2: 343–360. <https://doi.org/10.1111/j.1752-1688.2005.tb03740.x>.
- Soulsby, R. 1997. *Dynamics of marine sands*. London, UK: Telford.
- Staentzel, C., G. M. Kondolf, L. Schmitt, I. Combroux, A. Barillier, and J. N. Beisel. 2020. "Restoring Fluvial Forms and Processes by Gravel Augmentation or Bank Erosion Below Dams: A Systematic Review of Ecological Responses." *Science of the Total Environment* 706: 135743.
- Strickler, A. 1923. "Contributions to the Question of Velocity Formula and the Roughness Numbers for Rivers, Channels and Pipes." In *Mitteilung*, edited by C. Mutzner, vol. 16. Bern, Switzerland: Amt für Wasserwirtschaft. (in German).
- Surian, N., and M. Rinaldi. 2003. "Morphological Response to River Engineering and Management in Alluvial Channels in Italy." *Geomorphology* 50, no. 4: 307–326. [https://doi.org/10.1016/S0169-555X\(02\)00219-2](https://doi.org/10.1016/S0169-555X(02)00219-2).
- Talmon, A. M., N. Struiksma, and M. C. L. M. Van Mierlo. 1995. "Laboratory Measurements of the Direction of Sediment Transport on Transverse Alluvial-Bed Slopes." *Journal of Hydraulic Research* 33, no. 4: 495–517. <https://doi.org/10.1080/00221689509498657>.
- Tassi, P., T. Benson, M. Delinares, et al. 2023. "GAIA – A Unified Framework for Sediment Transport and Bed Evolution in Rivers, Coastal Seas and Transitional Waters in the TELEMAC-MASCARET Modelling System." *Environmental Modelling & Software* 159: 105544. <https://doi.org/10.1016/j.envsoft.2022.105544>.
- Thompson, D. M. 2006. "Did the Pre-1980 Use of In-Stream Structures Improve Streams? A Reanalysis of Historical Data." *Ecological Applications* 16, no. 2: 784–796.
- Vazquez-Amabile, G. G., and B. A. Engel. 2005. "Use of SWAT to Compute Groundwater Table Depth and Streamflow in the Muscatatuck River Watershed." *Transactions of the ASAE* 48, no. 3: 991–1003. <https://doi.org/10.13031/2013.18511>.
- Von Gunten, D., Y. Le Coarer, and F. Zaoui. 2018. Development of a Software Platform for Aquatic Habitat Models: HABBY/Développement d'une plate-forme de modèles d'habitats numériques: HABBY. Irstea, UR HYAX, Aix-en-Provence, France, & UR MALY, Villeurbanne, France. 11 pp. <https://hal.inrae.fr/hal-02608726>.
- Whiteway, S. L., P. M. Biron, A. Zimmermann, O. Venter, and J. W. A. Grant. 2010. "Do In-Stream Restoration Structures Enhance Salmonid Abundance? A Meta-Analysis." *Canadian Journal of Fisheries and Aquatic Sciences* 67, no. 5: 831–841.
- Williams, G. P., and M. G. Wolman. 1984. *Downstream Effects of Dams on Alluvial Rivers, Geological Survey Professional Paper 1286*. Washington, DC: U.S. Government Printing Office. <https://doi.org/10.3133/pp1286>.

Appendix A

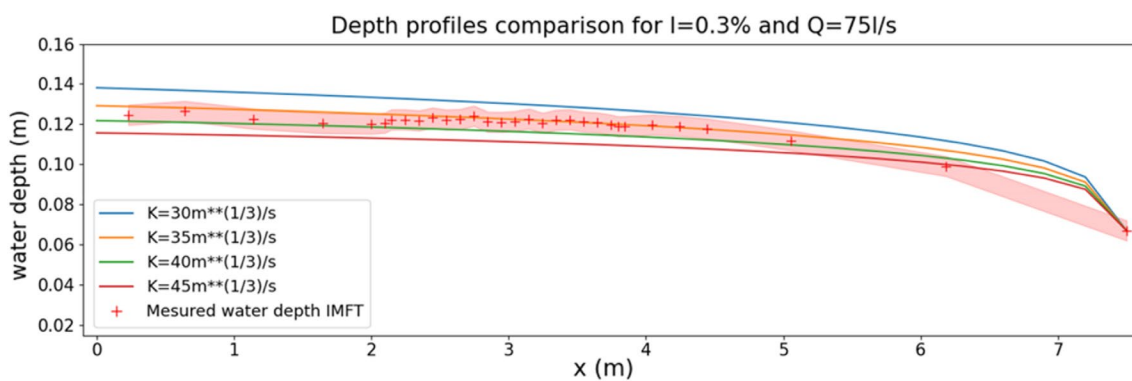
Meshes and Boundary Conditions

Meshes and boundary conditions used for the laboratory Cases H and I (a), and the prospective Scenarios O (b) and U (c). Eleven different meshes were constructed to model all configurations of the study. In the areas close to the boulders, the mesh is refined down to an element size of 0.5 mm.



Strickler Coefficient and Bedload Formula Choices

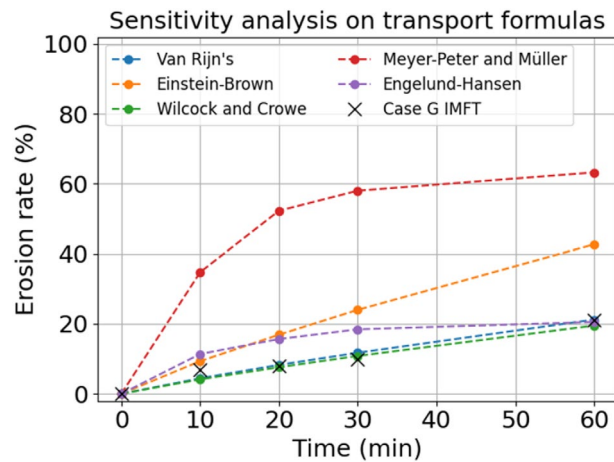
For these hydrodynamic simulations, we consider a flume in which there are only the fixed truncated cone-shaped elements with different Strickler coefficient values ($K = 30, 35, 40$ and $45 \text{ m}^{1/3}/\text{s}$). Comparisons of the PBIAS, RMSE, and RSR values indicate that the value $K = 35 \text{ m}^{1/3}/\text{s}$ provides the smallest deviations between simulations and measurements. For this value, the average deviation between observations and measurements is 2.7 mm (RMSE), and the PBIAS is less than 10% which indicates a very good performance of the model. For the other roughness coefficient in the replenishment area and in the boulder area, the Strickler formula ($K = 21 / d_{90}^{1/6}$; Strickler 1923) is used and then refined to match the erosion rate observed in the flume for Case G. The best results are obtained with $K = 50 \text{ m}^{1/3}/\text{s}$ in the replenishment area and $K = 18 \text{ m}^{1/3}/\text{s}$ in the boulders area.



Comparison between calculations and measurements of the longitudinal profile of the water height in the flume for a flow of 75L/s. Calibration process of the Strickler friction coefficient K (from 30 to $45 \text{ m}^{1/3}/\text{s}$ with an increment of $5 \text{ m}^{1/3}/\text{s}$).

Bedload Formula Sensitivity Analysis

A sensitivity analysis on the transport laws implemented in GAIA showed that Van Rijn's and Wilcock and Crowe's formulas are close to the experimental measurements. Van Rijn's law was chosen because it also allowed us to obtain temporal dynamics close to the observations.



Calibrated Parameters of Bedload Correction in GAIA Module

Parameter	Calibration possibilities	Recommended value in	
		GAIA	Calibrated values
Direction of the sediment transport	(Koch and Flokstra 1981)	—	Not used
	β_2 (Talmon, Struiksma and Van Mierlo 1995)	[0.85; 1.6]	0.85
Secondary flow effects on the direction of the bed shear stress	α_{sc}	[0.75; 1]	Not used
Skin friction correction	α_{ks} (Mendoza et al. 2017)	[3; 3.6]	4
Magnitude of the sediment transport	D_{50} (mm)	—	3.35
	Sediment density (kg/m ³)	2650	2650
	Critical shields parameter (—)	0.047	0.047
	β (Koch and Flokstra 1981)	1.3	1.3
	ϕ (Soulsby 1997)	[32°; 40°]	Not used
Bank failure algorithm	ϕ , sediment angle of repose (maxslope;°)	40°	40°

Errors Indication

The bias indicator (PBIAS) measures the average tendency of simulated data to be larger or smaller than their measured counterparts. The optimal value for PBIAS is 0, with low values indicating better accuracy for the simulations. Positive (respectively negative) values indicate an underestimation (respectively overestimation) bias of the model (Gupta et al. 1999). The PBIAS, in percentage, is calculated as:

$$PBIAS = \frac{\sum_{i=1}^n (a_i - p_i) \times 100}{\sum_{i=1}^n (a_i)} \quad (A.1)$$

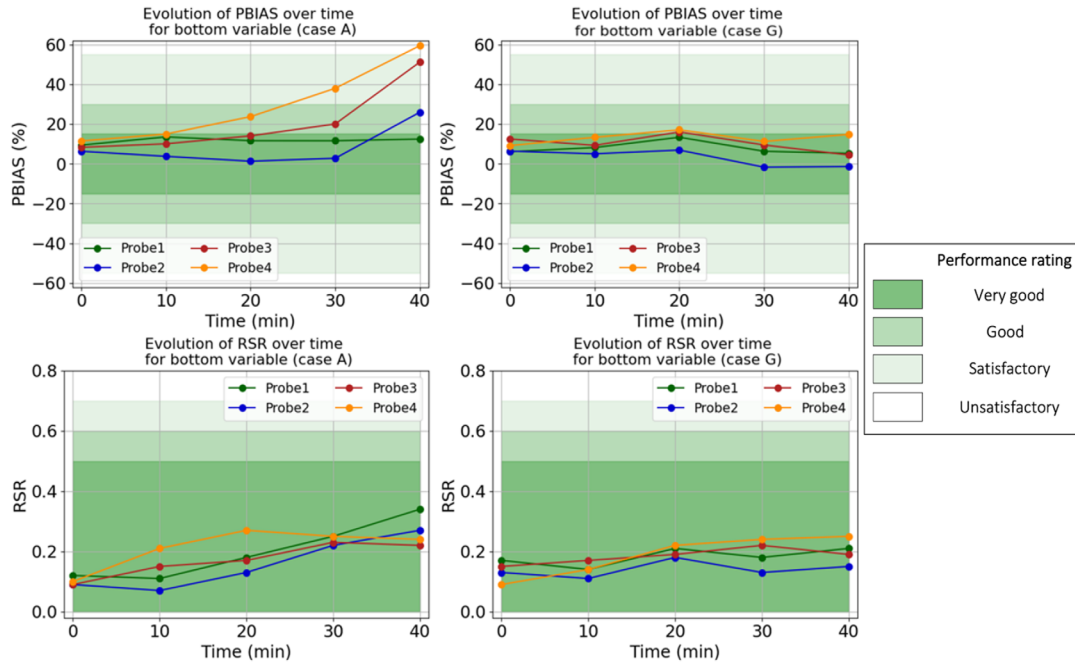
The model can be considered satisfactory if $PBIAS < 55\%$ for sediment for a monthly time step. The bias provides information on the deviation of the simulated data from the measured data but does not provide information on the magnitude of these deviations since the positive and negative values compensate each other. To account for this magnitude, the deviations are characterized by their mean squared, to make them positive. One commonly used error index statistic is the root mean square error (RMSE) (Chu and Shirmohammadi 2004; Singh et al. 2005; Vazquez-Amabile and Engel 2005):

$$RMSE = \sqrt{\frac{\sum_{i=1}^n (p_i - a_i)^2}{n}} \quad (A.2)$$

The RMSE indicates the error in units of the variable of interest, which facilitates analysis of the results. The closer the RMSE is to 0, the better is the model. However, to qualify for what is considered a sufficiently low value, a model evaluation statistic called the RMSE-observations standard deviation ratio (RSR) is recommended (Singh et al. 2005). The RSR normalizes the RMSE by dividing it by the standard deviation of the observations:

$$RSR = \frac{RMSE}{STDEV_{obs}} = \frac{\sqrt{\sum_{i=1}^n (p_i - a_i)^2}}{\sqrt{\sum_{i=1}^n (p_i - \bar{a})^2}} \quad (A.3)$$

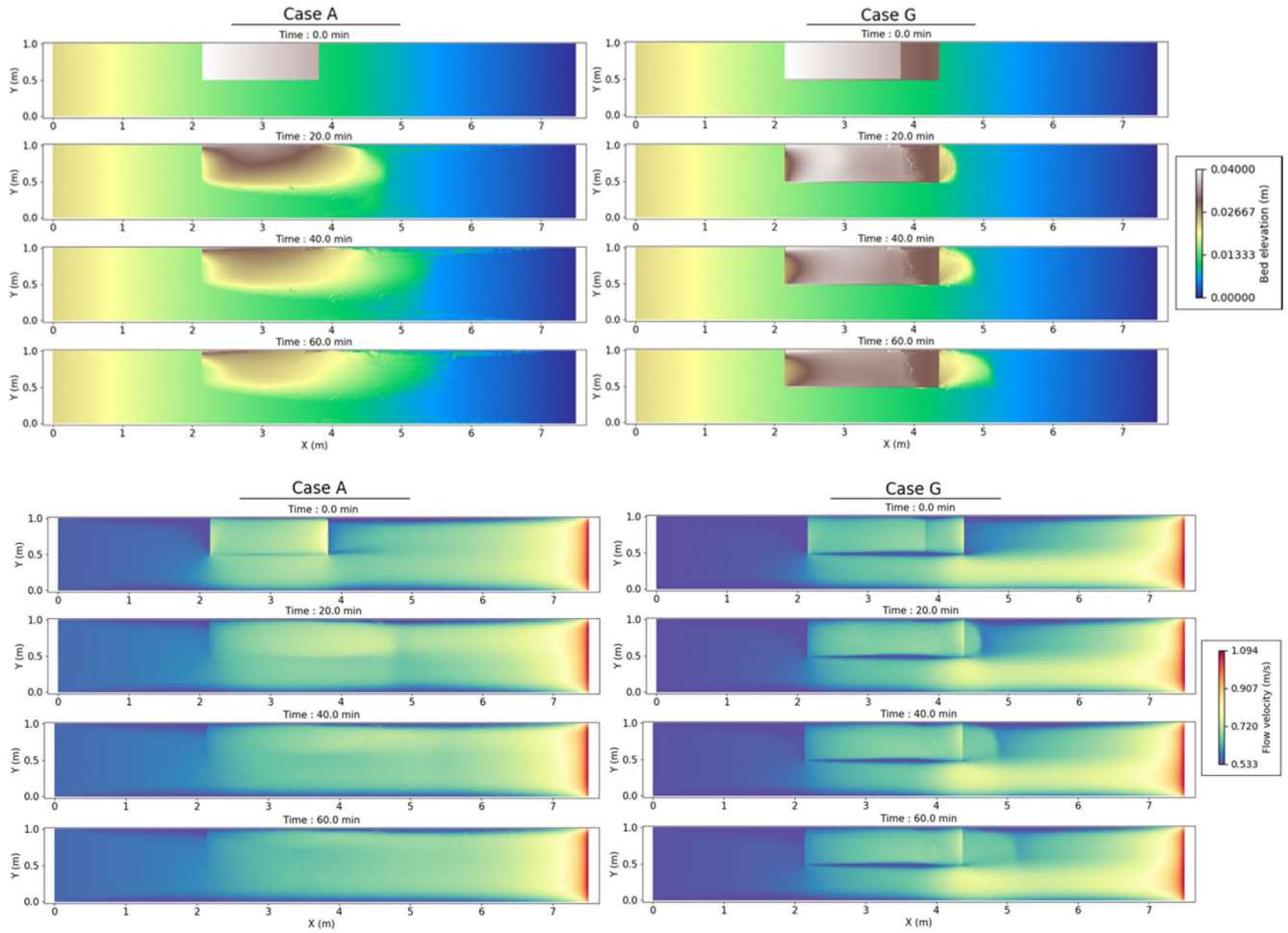
Singh et al. indicate that an RMSE value less than half the standard deviation is considered poor. Thus, when $RSR < 0.5$, the model performance is considered very good, and for $RSR < 0.7$, it is considered satisfactory for a monthly time step. In the study, we use a combination of visual verifications and criteria calculations to evaluate the results of the numerical model.



Spatiotemporal evolution of PBIAS and RSR of the bed evolution for each probe (probe 1: $y=0.9$ m; probe 2: $y=0.8$ m; probe 3: $y=0.7$ m; probe 4: $y=0.6$ m). The calculation is based on the measured flume bottom for cases A and G.

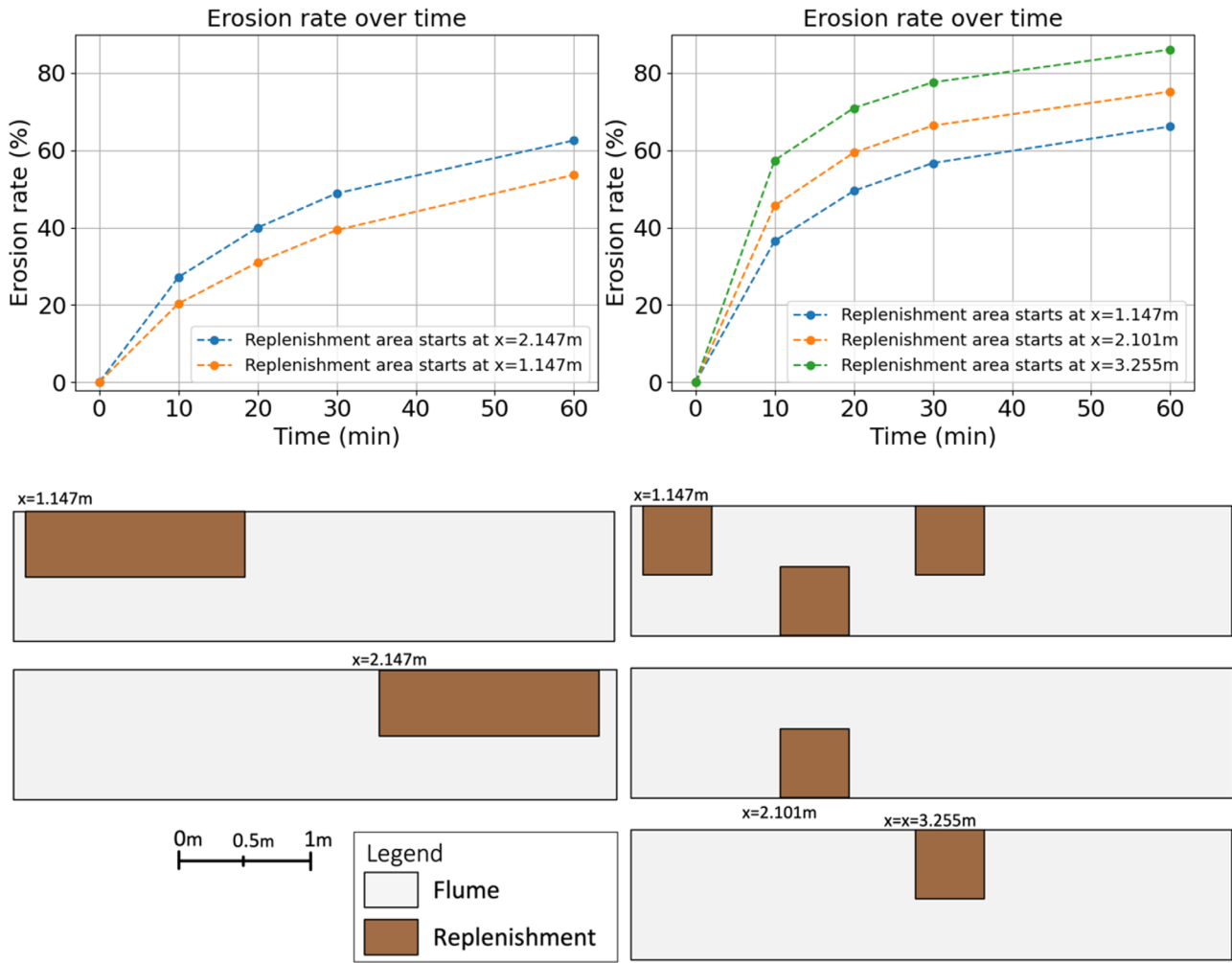
Comparison Between Cases A and G

Two-dimensional comparison of bed level and scalar velocity between Cases A and G. The 2D view of the bed level shows the shape of propagation of the replenishment deposit. In Case A, there is a lateral propagation that is prevented in Case G by the presence of a row of boulders placed longitudinally to the replenishment. The comparison of velocities shows that above the recharge the velocity is slightly lower in Case G than in Case A. Upstream of the replenishment deposit, the scalar velocity of the flow is lower for Case G. We can also note a very important acceleration of the flow approaching the downstream boundary condition; the flow regime is gradually varied along the channel. This observation is important because it means that there is an upstream and downstream effect on erosion of the sediment deposit. In studying prospective scenarios, these effects must also be considered.



Effect of the Gradually Varied Flow on the Replenishment

The flow regime is not uniform in the flume. As a result, there is a gradual acceleration of the flow along the flume, impacting the erosion rate of the replenishment deposit which is subject to upstream and downstream effects.



Comparison of erosion rates according to the position of the replenished deposit, and schematic drawing of the corresponding configurations